Mathematisches Forschungsinstitut Oberwolfach

Report No. 9/2019

DOI: 10.4171/OWR/2019/9

Mini-Workshop: Mathematical Aspects of Nonlinear Wave Propagation in Solid Mechanics

Organized by
Guiseppe Saccomandi, Perugia
Yasemin Şengül, Istanbul
Luigi Vergori, Perugia

3 March – 9 March 2019

Abstract. Nonlinear elastodynamics sets a plethora of challenging mathematical problems such as those concerning wave propagation in solids. Elastic vibrations and acoustic waves have been widely studied because of their applications in nondestructive tests of materials and structures, and, in recent times, several novel aspects of the theory of wave propagation in solids have blossomed thanks to the introduction of metamaterials and new technological devices.
The goal of this workshop was to bring together researchers with different backgrounds to discuss recent advances, and to stimulate future work.

Mathematics Subject Classification (2010): 74J30, 74J40, 74J10, 74J15, 74B20, 74B15, 74H10, 74H40, 74H55.

Introduction by the Organizers

The workshop *Mathematical Aspects of Nonlinear Wave Propagation in Solid Mechanics*, organised by Giuseppe Saccomandi (University of Perugia), Yasemin Şengül (Sabancı University, Istanbul) and Luigi Vergori (University of Perugia) was attended by 15 participants from 13 institutions, 12 of them European and one North American. This workshop was a nice blend of researchers with various backgrounds. There were mathematicians, physicists and engineers. Some of the participants are experimentalists, some are interested in qualitative and quantitative analysis of the PDEs governing wave propagation phenomena, and some others are focused on mathematical modelling. What joined all the participants was their will to share their knowledge in order to guide the future developments

of the research in the intriguing field of wave propagation in solids. In this respect, the workshop was successful.

The programme consisted of 15 talks and covered different aspects of nonlinear elastodynamics such us wave propagation in soft tissues, in viscoelastic and thermoviscoplastic materials, in metamaterials, and surface and bulk waves. Some talks posed the attention also to the mathematical modelling of brain matter, a current hot topic in nonlinear elasticity. The diversity of the topics and the participants stimulated fruitful discussions and gave rise to new collaborations.

In the following we include the abstracts in chronological order.

Acknowledgement: The MFO and the workshop organizers would like to thank the National Science Foundation for supporting the participation of junior researchers in the workshop by the grant DMS-1641185, "US Junior Oberwolfach Fellows".

Mini-Workshop: Mathematical Aspects of Nonlinear Wave Propagation in Solid Mechanics

Table of Contents

Giuseppe Saccomandi
Non-linear elasticity: a disputatio 581

Athanasios E. Tzavaras (joint with Theodoros Katsaounis, Min-Gi Lee)
Instability leading to localization in high strain-rate deformations of metals 584

Anastasiia O. Krushynska
Waves in elastic and dissipative acoustic metamaterials 587

Michel Destrade
Small-amplitude elastic waves in soft matter 589

Miroslav Bulíček
PDE analysis of a class of thermodynamically compatible viscoelastic rate-type fluids with stress-diffusion 592

Yasemin Şengül
Viscoelasticitiy with limited strain: traveling waves and the Cauchy problem 596

Husnu Ata Erbay (joint with S. Erbay, A. Erkip)
One-dimensional nonlinear waves in nonlocal elastic materials 598

Katrin Grunert (joint with J. A. Carrillo, H. Holden)
Lipschitz metrics for nonlinear PDEs 599

Gianmarco Pinton
Shear shock wave propagation in soft solids and the brain: ultrasound imaging and simulations 601

Ilya Peshkov
Riemann-Cartan geometry as a framework for modeling of nonlinear dispersive waves in solids 601

Valentina Balbi
The mechanics of a twisted brain 602

Andrea Nobili (joint with Enrico Radi, Gennadi Mishuris)
Shear wave pattern in the elastodynamic of a cracked half-space with microstructure 604

Yibin Fu
Traveling and standing solitary waves in a prestressed coated elastic half-space. 607

Jacopo Ciambella
Large strain viscoelastic response of fibre-reinforced materials 608
Luigi Vergori
Linearly polarised waves in pre-strained elastic materials 610

Abstracts

Non-linear elasticity: a disputatio

Giuseppe Saccomandi

The theory of nonlinear elasticity is central in continuum mechanics. On the one hand nonlinear elasticity exhaustively describes the statics and dynamics of any Noll's simple material; on the other, it provides thorough descriptions of the nonlinear behaviour of solids.

Despite its mathematical elegance and versatility, the theory of nonlinear elasticity shows a challenging *hauptproblem*: the determination of the most appropriate strain energy function to describe the behaviour of a given material. Several important results have been obtained in this direction, but scholars are yet groping in the dark. The main difficulty stands in the fact that the strain energy density can be chosen in an infinite set of functional forms, and any reasonable mathematical restriction imposed to such a set does not limit significantly the choice. We can then claim that in contrast to the linear theory of elasticity, in which the functional form of the strain energy is fixed up to some constants, in the nonlinear theory there is a sort of *Pandora's box* containing the infinitely many strain energy functions which are, in principle, appropriate for describing the material response.

Unfortunately, the choice of the strain energy function is not the sole problem in nonlinear elasticity. Indeed, once the functional form for the strain energy density has been chosen, nonlinearities may generate problems with fitting the experimental data and hence with the determination of the material parameters. Specifically, there may exist multiple sets of optimal material parameters for a given set of data. As reasonable to expect, the non-uniqueness of the optimal material parameters may lead to completely different solutions of a given boundary-value problem [7].

These difficulties might discourage even the willingest researcher and make them give up the use of a so complex theory. It seems that the efforts necessary to draw up interesting and sound results are out of all proportion to the resulting benefit.

To somehow confirm the last two sentences, let us consider the simple torsion of an elastic cylinder. This is a static deformation presented in details in several textbooks (see [1], for instance), and is widely adopted in experimental setups. In the linearized theory of elasticity the relationship between the amount of twist, say τ, and the couple M necessary to produce it is given by

$$M = \frac{\pi}{2}\mu\tau a_o^4, \tag{1}$$

with μ being the *constant* infinitesimal shear modulus, and a_o the radius of the cylinder. The modern machines used in simple torsion tests can measure couples of the order of 10^{-9} N/m.

Shear deformations and shearing motions are at the basis of the usual palpation process of using the hands to check the body, especially while perceiving a disease or illness. Such a process have been turned to an objective and quantitative methodology by elastography. To give an idea of the measure of how nonlinear

elasticity can help the modern elastography to detect suspicious masses, assume that inside the cylinder there is a coaxial inclusion of radius $a_i \ll a_o$ and made of an elastic material with shear modulus $\mu_i > \mu$. The difference between the couples necessary to produce a given amount of twist with or without the inclusion is easily found to be

$$\Delta M = \frac{\pi}{2}\mu\tau a_i^4 \left(\frac{\mu_i}{\mu} - 1\right). \tag{2}$$

So, if the sample has radius $a_o = 3$ cm and contains a cylindrical inclusion with radius $a_i = 0.3$ mm which is ten times stiffer than the bulk (namely $\mu_i/\mu = 10$), from (2) we deduce that ΔM is of order 10^{-6} N/m. Such a discrepancy in the couples is easily detectable by the current technology.

At this stage, it is natural to wonder whether the nonlinear theory of elasticity may improve this measurement and allow the detection of smaller inclusions. The deformation at hand is a universal solution for incompressible elastic materials and thus formula (1) can be easily generalized to the nonlinear case. Within the *weakly* nonlinear theory one obtains

$$M = \frac{\pi}{2}\mu\tau a_o^4 \left(1 + \frac{\gamma\tau^2}{3}a_o^2\right), \tag{3}$$

where γ is a coefficient accounting for the nonlinearities. As a consequence of not neglecting the nonlinear effects, the extra term

$$(\Delta M)_{nl} = \frac{\pi}{3}\tau^3 a_i^6 \left(\frac{\mu_i\gamma_i}{\mu} - \gamma\right),$$

with γ_i being the coefficient of nonlinearity of the inclusion, has to be added to the right hand side of (2). Unless the amount of twist is very large, $(\Delta M)_{nl}$ is of the order 10^{-9} N/m and thus at the borders of the current technological precision. Thus one might think that resorting to an involved theory such as nonlinear elasticity does not pay off.

Clearly, this is a rushed conclusion. In some pathologies the change of the material properties of soft tissues may be so abrupt that the weakly nonlinear theory of elasticity is not appropriate to give a satisfactory depiction of the reality. For instance, consider the degradation of soft tissue causing the stiffening of the material the tissue is made of. Guided by the analysis in [8], one can adopt the Gent model for the strain energy function,

$$W = -\frac{\mu}{2}J_m \ln\left(1 - \frac{I_1 - 3}{J_m}\right), \tag{4}$$

to studying the stiffening of the soft tissue. In (4) μ is, as before, the infinitesimal shear modulus, $I_1 = \mathrm{tr}(\boldsymbol{F}\boldsymbol{F}^T)$, with $\boldsymbol{F}$ being the deformation gradient, and $J_m > 0$ is constitutive parameter which imposes an upper bound to the extensibility of the chain composing the macromolecular network of the soft tissue. The smaller J_m is, the stiffer the material is [10]. When the strain energy is modelled as in (4),

the relationship between the couple M and the amount of twist τ in a torsion test reads [6]

$$M = -\mu\pi \frac{J_m a_o^2}{\tau} \left[1 + \frac{J_m}{\tau^2 a_o^2} \ln\left(1 - \frac{\tau^2 a_o^2}{J_m} \right) \right]. \tag{5}$$

In the limit as $J_m \to \infty$ equation (5) reduces to (1), while for small values of J_m the couple M necessary to produce a small amount of twist is very large. As easy to deduce from (1), the latter situation cannot be predicted by the linearized theory of elasticity.

There are other reasons why it is unavoidable to use the nonlinear theory of elasticity. Many experimental evidences [5, 9, 4] reveal the coupling of deformation modes, a phenomenon which cannot be described by the linear theory.

In view of these observations it is worth pursuing the rocky path to finding the *most appropriate* strain energy function of a given material. This task is very challenging, but some steps toward the desired goal have been made. In [3] we have developed a method which provides models that describe the experimental data with a very low quantitative relative error, and shows that the theory of nonlinear elasticity is much more *robust* than seemed at first sight.

Acknowledgements

The works mentioned here were supported by Fondi di Ricerca di Base Università degli Studi di Perugia and by the GNFM of the Istituto Nazionale di Alta Matematica.

References

[1] R.J. Atkin, N. Fox, *An introduction to the theory of elasticity*, Courier Corporation (2013).

[2] J.M. Ball, *Some open problems in elasticity*, in *Geometry, mechanics, and dynamics* (pp. 3–59). Springer, New York, NY, (2002).

[3] M. Destrade, G. Saccomandi, I. Sgura, *Methodical fitting for mathematical models of rubber-like materials*, Proceedings of the Royal Society A: Mathematical, Physical and Engineering Sciences **473** (2017), 20160811.

[4] M. Destrade, E. Pucci, G. Saccomandi, *Proper generalization of the Zabolotskaya equation to all incompressible isotropic elastic solids*, submitted.

[5] R. De Pascalis, M. Destrade, G. Saccomandi, *The stress field in a pulled cork and some subtle points in the semi-inverse method of nonlinear elasticity*, Proceedings of the Royal Society A: Mathematical, Physical and Engineering Sciences **463** (2007), 2945–2959.

[6] C.O. Horgan, G. Saccomandi, *Simple torsion of isotropic, hyperelastic, incompressible materials with limiting chain extensibility*, Journal of Elasticity **56**(2) (1999), 159–170.

[7] R.W. Ogden, G. Saccomandi, I. Sgura, *Fitting hyperelastic models to experimental data*, Computational Mechanics **34**(6) (2004), 484–502.

[8] R.W. Ogden, G. Saccomandi, *Introducing mesoscopic information into constitutive equations for arterial walls*, Biomechanics and modeling in mechanobiology **6**(5) (2007), 333–344.

[9] E. Pucci, G. Saccomandi, *Secondary motions associated with anti-plane shear in nonlinear isotropic elasticity*, The Quarterly Journal of Mechanics and Applied Mathematics **66**(2) (2013), 221–239.

[10] G. Puglisi, G. Saccomandi, *The Gent model for rubber-like materials: an appraisal for an ingenious and simple idea*, International Journal of Non-Linear Mechanics **68** (2015), 17–24.

Instability leading to localization in high strain-rate deformations of metals

Athanasios E. Tzavaras
(joint work with Theodoros Katsaounis, Min-Gi Lee)

Shear bands are narrow zones of intensely localized shear that are formed during the high speed plastic deformations of metals and often precede rupture [6, 1]. A popular model, studied in both the mechanics and mathematics literature, is

$$\begin{aligned} v_t &= \kappa\theta_{xx} + \sigma_x, \\ \theta_t &= \sigma\gamma_t, \\ \gamma_t &= v_x, \end{aligned} \tag{1}$$

$$\sigma = f(\theta,\gamma,u) = \theta^{-\alpha}\gamma^m u^n\,, \qquad u = \gamma_t. \tag{2}$$

It describes the adiabatic plastic shearing of a thermoviscoplastic material, where (2) may be viewed as a yield surface or a plastic flow rule, and encompasses the basic mechanisms entering in theories for the explanation of shear bands [6, 1]. The variable v is the shear velocity, γ the plastic strain, θ the temperature and σ the stress. The parameters $\alpha > 0$, $m > 0$ and $n > 0$ measure respectively the degrees of thermal softening, strain hardening and strain-rate hardening; typically $n \ll 1$, [1], and the parameters (α, m, n) are restricted to the range

$$\begin{aligned} &\alpha > 0 \quad \text{(thermal softening)} && m > -1 \text{ (strain softening/hardening)}, \\ &-\alpha + m < 0 \quad \text{(loss of hyperbolicity)} && n \geq 0 \quad \text{(strain rate sensitivity)}. \end{aligned}$$

An adiabatic hypothesis, $\kappa = 0$, is quite reasonable for studying the initial development of shear bands and leads to the system of partial differential equations

$$\begin{aligned} v_t &= \partial_x\Big(\theta^{-\alpha}\gamma^m v_x^n\Big), \\ \theta_t &= \theta^{-\alpha}\gamma^m v_x^{n+1} \\ \gamma_t &= v_x, \end{aligned} \tag{3}$$

subject to velocity boundary conditions.

We first investigate the stability of the uniform shearing solutions. Since these are time-dependent, the linearized theory has to account for the behavior of non-autonomous systems. We present a rigorous theory that illustrates the behavior of linearized modes around the time dependent base solutions, in the spirit of [2] and developed in [5]. The functions

$$\gamma_s^*(t) = t + \gamma_0, \quad \theta_s^*(t) = c^{\frac{1}{1+\alpha}}(t+\gamma_0)^{\frac{1+m}{1+\alpha}}\,, \quad \sigma_s^*(t) = c^{\frac{-\alpha}{1+\alpha}}(t+\gamma_0)^{\frac{-\alpha+m}{1+\alpha}}\,, \tag{4}$$

where $c = \frac{1+\alpha}{1+m}$, capture the leading order response of the uniform shearing solutions. New dependent variables $u(t,x)$, $\Gamma(t,x)$, $\Theta(t,x)$ and $\Sigma(t,x)$ are introduced,

$$u(t,x) = v_x(t,x)\,, \quad \hat\Gamma(t,x) = \frac{\gamma(t,x)}{\gamma_s^*(t)}, \quad \hat\Theta\big(t,x\big) = \frac{\theta(t,x)}{\theta_s^*(t)}, \quad \hat\Sigma(t,x) \quad = \frac{\sigma(t,x)}{\sigma_s^*(t)}\,, \tag{5}$$

that are called in [2] *relative perturbations* and lead to studying the system

$$\begin{aligned} &\partial_\tau U = \Sigma_{xx},\\ &\partial_\tau \Gamma = \frac{c}{\tau}\Big(U-\Gamma\Big), \qquad \text{where} \quad \Sigma = \Theta^{-\alpha}\Gamma^m U^n.\\ &\partial_\tau \Theta = \frac{1}{\tau}\Big(\Sigma U-\Theta\Big), \end{aligned} \tag{6}$$

The uniform shearing solution is mapped to the equilibrium $(1,1,1)$ via the transformation (5).

The linearized system around the equilibrium state $(1,1,1)$ takes the form:

$$\begin{aligned} &\partial_\tau \bar{u} = n\bar{u}_{xx} + m\bar{\gamma}_{xx} - \alpha\bar{\theta}_{xx},\\ &\partial_\tau \bar{\gamma} = \frac{c}{\tau}(\bar{u}-\bar{\gamma}),\\ &\partial_\tau \bar{\theta} = \frac{1}{\tau}\Big((n+1)\bar{u} + m\gamma - (\alpha+1)\bar{\theta}\Big), \end{aligned} \tag{7}$$

it is non-autonomous, and presents relaxation and cross-diffusional effects. The boundary condition yields

$$\bar{\sigma}_x(\tau,0) = \bar{\sigma}_x(\tau,\pi) = 0, \quad \int_0^\pi \bar{u}(t,x)\,dx = 0. \tag{8}$$

The system (7) can be diagonalized and, even if it is non-autonomous, the eigenvalues are strictly separated. This property together with a theory for stability of such problems (see [5]) allows to conclude :

- the equilibrium $(1,1,1)$ is asymptotically stable when $-\alpha+m+n>0$,
- the equilibrium $(1,1,1)$ is unstable in the region $-\alpha+m+n<0$.

The instability has some analogies to the well-known Turing instability.

In the unstable regime $-\alpha+m+n<0$, at the initial stage, unstable modes begin to grow and this process is captured by the linearized problem. However, the next stage of localization lies within the realm of nonlinear analysis. The question arises how the high frequency oscillations resulting from Hadamard instability interact with the nonlinearity and the viscosity to form a coherent structure. Insight is offered by investigating self-similar solutions, see [3] and [4].

Exploiting the scaling invariance of (3) (or (6)), we seek a class of self-similar solutions of the form

$$\begin{aligned} &\gamma(t,x) = t^a\Gamma\big(x\,t^\lambda\big), \quad v(t,x) = t^b V\big(x\,t^\lambda\big), \qquad \theta(t,x) = t^c\Theta\big(x\,t^\lambda\big),\\ &\sigma(t,x) = t^d\Sigma\big(x\,t^\lambda\big), \quad u(t,x) = t^{a-1}U\big(x\,t^\lambda\big), \end{aligned} \tag{9}$$

where $\lambda>0$ and (α,m,n) take values in the range $-\alpha+m+n<0$. Parabolic systems (such as (3)) usually admit diffusing self similar solutions, constant on lines $\xi = \frac{x}{t^\rho}$. By insisting here on $\lambda>0$, the solutions (9) will propagate information on lines $xt^\lambda = const$ that focus around the origin. We seek that the profiles (V,Σ,Γ,Θ) are localizing. We call a self-similar function

$$f(t,x) = t^b F(xt^\lambda)\,, \quad \text{with } F(-\xi) = F(\xi) \text{ and } \lambda>0 \tag{10}$$

localizing if it has the asymptotic behavior

$$F(\xi) = O(\xi^p) \quad \text{as } \xi \to \infty \tag{11}$$

and satisfies that $p < 0$ when $b > 0$ while $p > 0$ when $b < 0$. Under this definition, when $f(t, 0)$ grows then $f(t, x)$ grows at a slower rate when $x \neq 0$, while when $f(t, 0)$ decays then $f(t, x)$ decays at a slower rate at $x \neq 0$. We will call a self-similar function with an odd-profile $F(-\xi) = -F(\xi)$ localizing when its derivative $f_x(t, x)$ has the aforementioned behavior.

The *ansatz* (9) leads to solving the system

$$\begin{aligned} V'(\xi) &= U(\xi), \\ \Sigma'(\xi) &= bV(\xi) + \lambda\xi U(\xi), \\ a\Gamma(\xi) + \lambda\xi\Gamma'(\xi) &= U(\xi), \\ c\Theta(\xi) + \lambda\xi\Theta'(\xi) &= \Sigma(\xi)U(\xi), \\ \Sigma(\xi) &= \Theta(\xi)^{-\alpha}\Gamma(\xi)^m U(\xi)^n, \\ \Gamma(0) = \Gamma_0 > 0, \quad U(0) = U_0 > 0, \quad V(0) &= U'(0) = 0 \end{aligned} \tag{12}$$

for $\xi \in [0, \infty)$. This is a system of singular ordinary differential equations for $(V, \Sigma, \Gamma, \Theta)$ with U defined by inverting $(12)_5$. The main result in [4] is the construction of solutions to (12), which turn out to exhibit localizing behavior in space as time evolves. This is is justified by analysis of the qualitative properties of the solutions (9) as well as by numerical calculation of the associated profiles. The method of proof proceeds as follows: The system (12) is singular and non-autonomous. Nevertheless, the singularity at $\xi = 0$ can be resolved and (12) is desingularized using again the scale-invariance properties. Furthermore, upon introducing a series of nonlinear transformations, the construction of solutions to (12) is reduced to constructing a heteroclininc connection for a system of four ordinary differential equations. The resulting system is singular for the parameter $n << 1$ and the latter construction is effected by using the geometric theory of singular perturbations, see [4].

References

[1] R.J. Clifton, *High strain rate behaviour of metals*, Applied Mechanics Reviews **43** (1990), S9-S22.

[2] C. Fressengeas and A. Molinari , *Instability and localization of plastic flow in shear at high strain rates*, J Mech Phys Solids **35** (1987), 185-211.

[3] Th. Katsaounis, J. Olivier, and A.E. Tzavaras, *Emergence of coherent localized structures in shear deformations of temperature dependent fluids*, Archive for Rational Mechanics and Analysis **224** (2017), 173–208.

[4] M.-G. Lee, Th. Katsaounis, and A.E. Tzavaras, *Localization in adiabatic shear flow via geometric theory of singular perturbations*, J Nonlinear Sci (2019). https://doi.org/10.1007/s00332-019-09538-3

[5] M.-G. Lee and A.E. Tzavaras, *Dynamic shear band formation in high strain-rate plasticity of metals*, (in preparation).

[6] C. Zener and J.H. Hollomon, *Effect of strain rate upon plastic flow of steel.* J. Appl. Physics, **15** (1944), 22–32.

Waves in elastic and dissipative acoustic metamaterials

Anastasiia O. Krushynska

The concept of exploiting architecture to alter material behaviour and recent advances in additive manufacturing techniques have formed a foundation for developing innovative materials with unprecedented properties – metamaterials – paving the way to previously unforeseen multifunctional applications in acoustics, (bio)mechanics, optics, electro-magnetism, etc. [1]. Metamaterials are rationally designed composites formed by rationally tailored building blocks that exhibit effective medium properties going far beyond those of their ingredients [2]. In mechanics and acoustics, these are advanced mechanical and acoustic properties, including negative effective stiffness or mass density, topologically protected one-way wave propagation, perfect absorption, programmability or chirality, among others [1, 2, 3]. Acoustic metamaterials typically have a periodic structure of crystallographic lattices or are hierarchically organized. They can be realized at broad dimension scales, ranging from nanometers to several meters, and operate at frequencies extending from GHz down to infrasound or frequencies of seismic waves (<10 Hz).

Linear elastic metamaterials. A common acoustic metamaterial consists of a host and a periodic set of (non-)resonant scatterers. In case of linear elastic behaviour of the constituent materials, such a structure results in wave folding at the boundaries of the high-symmetry directions in the reciprocal space [4] and causes geometric dispersion of waves. The latter refers to the phenomenon of frequency-dependent phase (or group) wave velocity at a boundary or an interface [5, 6]. The geometric dispersion leads to the coupling of waves propagating in the host at interfaces with scatterers. If the contrast in longitudinal and shear wave velocities of constituents is high, a scattered wave field can cancel incident waves. The frequencies at which this phenomenon occurs are known as frequency band gaps.

Due to a structural periodicity, the wave dispersion in a metamaterial can be analysed by considering a representative building block and applying Floquet-Bloch periodic conditions on its boundaries [4, 7]. The related eigenfrequency problem can then be solved for real values of the wavevector along the boundary of the irreducible Brillouin zone. Solutions constitute infinite non-condensed sets of eigenfrequencies corresponding to pass bands of propagating waves. If they are represented graphically with the wavevector values along a horizontal axis and frequencies along the vertical axis, these eigenfrequencies form a dispersion spectrum, in which band gaps are recognized as frequency regions without pass bands.

From the physical point of view, a dispersion spectrum cannot have any gaps, as each mode should continuously span from zero to infinite frequency (see e.g. [8] and the references therein). To solve this issue and complete the spectrum of a metamaterial, one needs to include into consideration non-propagating modes with imaginary and complex values of the wavevector [9]. Thus, another definition

for a band gap is that it is a frequency region with only non-propagating modes. The trends (shape) of non-propagating bands can suggest a physical mechanism of band-gap generation [10]. The knowledge of a full dispersion spectrum including non-propagating modes can also be useful to estimate the level of wave attenuation within band gaps [9].

Dissipative metamaterials. If either a host or scatterers (or both) are made of materials with non-negligible energy dissipative behaviour, the situation becomes more complicated, since apart from the geometric dispersion, the material dispersion takes place. Due to the presence

of losses, propagating waves attenuate during propagation that can be taken into account by a non-zero imaginary part of the wavevector. Thus, a dispersion spectrum contains only bands with complex-values wavevectors, and the introduced notion of a band gap, strictly speaking, becomes meaningless [9]. Material dispersion in dissipative materials can be exploited to achieve enhanced wave attenuation or suppress the resonant-induced wave scattering [9].

New trends in the metamaterial design. One of recent tendencies in the design of mechanical metamaterials is based on the enriched continuum model at the building block level. Such a model can be obtained e.g. by introducing chiral effects to enable the coupling between displacement and rotation [2, 11]. In our works, we translate this idea into the wave dynamics domain by exploiting a known property of regular tensegrity units to undergo twisting under axial loading. In this way, we have developed an acoustic metamaterial with coupled translation-rotation modes. By tailoring geometry of the twisted components, we have obtained very light-weight configurations with extremely broadband low-frequency band gaps and advanced energy absorption ratio [13]. An additional benefit is a tunability feature allowing to control the effective material stiffness by varying the level of pre-strain in incorporated strings [12, 13].

Finally, we mention another strategy to induce omnidirectional wave attenuation performance in three-dimensional acoustic metamaterials. It implies a combination of a phononic plate of an arbitrary configuration with a rotation-symmetric zincblende lattice unit [14]. Such a hybrid designs activates a band-gap mechanism attributed solely to the material architecture, rather than to a specific choice of geometric or material properties. We have shown that the hybrid metamaterials can efficiently attenuate low-frequency waves by means of a few materials building blocks and exploiting structural damping inherently present in realistic materials.

Acknowledgements. The works mentioned here were done in close collaboration with Eindhoven University of Technology (the Netherlands), University of Turin (Italy), University of Salerno (Italy), University of Wisconsin-Madison (U.S.A.), and University of Trento (Italy). The author expresses sincere appreciation to her colleagues at these universities for their substantial contribution to this research.

References

[1] J. U. Surjadi, L. Gao, H. Du, et.al., *Mechanical metamaterials and their engineering applications*, Adv. Eng. Mat. **21**(3) (2019), 1800864.

[2] M. Kadic, G.W. Milton, M. van Hecke, M. Wegener, *3D metamaterials*, Nat. Rev. Phys. **1** (2019), 198–210.

[3] A.O. Krushynska, F. Bosia, M. Miniaci, N.M. Pugno, *Spider web-structured labyrinthine acoustic metamaterials for low-frequency sound control*, New J. Phys. **19** (2017), 105001.

[4] L. Brillouin, *Wave propagation in periodic structures*, McGraw-Hill (1946).

[5] V.V. Meleshko, A.A. Bondarenko, S.A. Dovgiy, A.N. Trofimchuk, G.J.F. van Heijst, *Elastic waveguides: History and the state of the art. I*, J. Math. Sci. **162** (2009), 99–120.

[6] V.V. Meleshko, A.A. Bondarenko, A.N. Trofimchuk, R.Z. Abasov, *Elastic waveguides: History and the state of the art. II*, J. Math. Sci. **167** (2010), 197–216.

[7] A.O. Krushynska, V.G. Kouznetsova, M.G.D. Geers, *Towards optimal design of locally resonant acoustic metamaterials*, J. Mech. Phys. Solids **71** (2014), 179–196.

[8] A.A. Krushynska, V.V. Meleshko, *Normal waves in elastic bars of rectangular cross section*, J. Acoust. Soc. Am. **129**(3) (2011), 1324–1335.

[9] A.O. Krushynska, V.G. Kouznetsova, M.G.D. Geers, *Visco-elastic effects on wave dispersion in three-phase acoustic metamaterials*, J. Mech. Phys. Solids **96** (2016), 29–47.

[10] A.O. Krushynska, M. Miniaci, F. Bosia, N.M. Pugno, *Coupling local resonance with Bragg band gaps in single-phase mechanical metamaterials*, Extr. Mech. Lett. **12** (2017), 30–36.

[11] I. Fernandez-Corbaton, C. Rockstuhl, P. Ziemke, P. Gumbsch, et.al., *New twists of 3D chiral metamaterials*, Adv. Mat. (2019), 1807742.

[12] A. Amendola, A. Krushynska, C. Daraio, N.M. Pugno, F. Fraternali, *Tuning frequency band gaps of tensegrity mass-spring chains with local and global prestress*, Int. J. Solids Struct. **155** (2018), 47–56.

[13] A.O. Krushynska, A. Amendola, F. Bosia, C. Daraio, N.M. Pugno, F. Fraternali, *Accordion-like metamaterials with tunable ultra-wide low-frequency band gaps*, New. J. Phys. **20**(7) (2018), 073051.

[14] A.O. Krushynska, P. Galich, F. Bosia, N.M. Pugno, S. Rudykh, *Hybrid metamaterials combining pentamode lattices and phononic plates*, Appl. Phys. Lett. **113**(20) (2018), 201901.

Small-amplitude elastic waves in soft matter

Michel Destrade

Introduction

Biological soft tissues and soft gels are difficult to study and model mathematically. Bioengineers often see them as engineering materials and try to evaluate their mechanical properties with standard testing protocols, such as tensile testing, simple shear, torsion, etc. These processes are destructive for tissues, as a sample is taken out of the body and placed in a device. The resulting measured parameters and models are expected to be very different from their in vivo counterparts.

To test soft tissues properly, non-destructively, and non-invasively, we can rely on elastic waves. We can study the influence of pre-stress on their speed and obtain the nonlinear elastic parameters by inverse analysis. This idea forms the basis of the theory of *acousto-elasticity*, which can be dated back to early works of Brillouin, and has been used successfully in the past for "hard" elastic solids such as rocks and metals.

Here we explore the extension of acousto-elasticity to "soft" elastic solids, which can be subjected to large deformations in service. We look at theoretical, numerical, experimental, and even clinical results, generated in particular on gels, brain, breast, and skin.

Destructive testing of soft matter

To test soft biological tissue, we can rely on existing testing protocols for soft solids such as rubber. Hence we can, in principle, stretch, twist, shear, inflate, and bend them, but in practice it is not always possible to obtain reliable and accurate measurements. Soft tissues *ex vivo* have very different properties from when they are "in service", because of cell death, dehydration, release of residual stresses and many other factors. Moreover, they do not all lend themselves to be tested in those protocols.

For instance, brain matter is extremely soft and fragile, and cannot be tested as a thin membrane, which rules out the inflation, pure shear, and dog-bone tensile tests. It cannot be gripped or attached by hooks, and must be glued instead. That limitation rules out cylinder tension and compression tests, as inhomogeneous local effects then develop near the attached platens and makes modelling difficult. But within this limitation, *simple shear* and *torsion* do work reasonably well, see Figures 1(a)-(d).

Experimentally, we find linear relationships between the Cauchy shear stress component T_{12} and the amount of shear K, and between the torque τ and the twist ϕ, when we test pig brain samples in simple shear and torsion, see Figures 1(e)-(f). Using the general expressions

$$T_{12} = 2\left(\frac{\partial W}{\partial I_1} + \frac{\partial W}{\partial I_2}\right) K, \qquad \tau = 4\pi\phi \int_0^a r^3 \left(\frac{\partial W}{\partial I_1} + \frac{\partial W}{\partial I_2}\right) dr, \tag{1}$$

(where r is the radial distance and a is the radius of the twisted cylinder), we see that the Mooney-Rivlin strain energy density W_{MR} is particularly appropriate,

$$W_{\mathrm{MR}} = \tfrac{1}{2}C_1(I_1 - 3) + \tfrac{1}{2}C_2(I_2 - 3), \tag{2}$$

(where $C_1 > 0$, $C_2 > 0$ are constants, and $I_1 = \operatorname{tr}\mathbf{C}$, $I_2 = \operatorname{tr}(\mathbf{C}^{-1})$ are the first two principal invariants of the right Cauchy-Green deformation tensor $\mathbf{C}$), because it provides indeed exact linear relationships.

Non-destructive testing with acousto-elasticity

To test soft tissues *in situ*, we may rely on *acousto-elasticity theory*, which gives the relationship between the speed of an elastic wave and the deformation of the soft solid.

For example, a homogeneous plane wave of small amplitude travels in an incompressible solid of mass density ρ and strain energy density W with speed v given by the formula

$$\rho v^2 = \left(\lambda_2 \frac{\partial W}{\partial \lambda_2} - \lambda_1 \frac{\partial W}{\partial \lambda_1}\right) \frac{\lambda_2^2}{\lambda_2^2 - \lambda_1^2}, \tag{3}$$

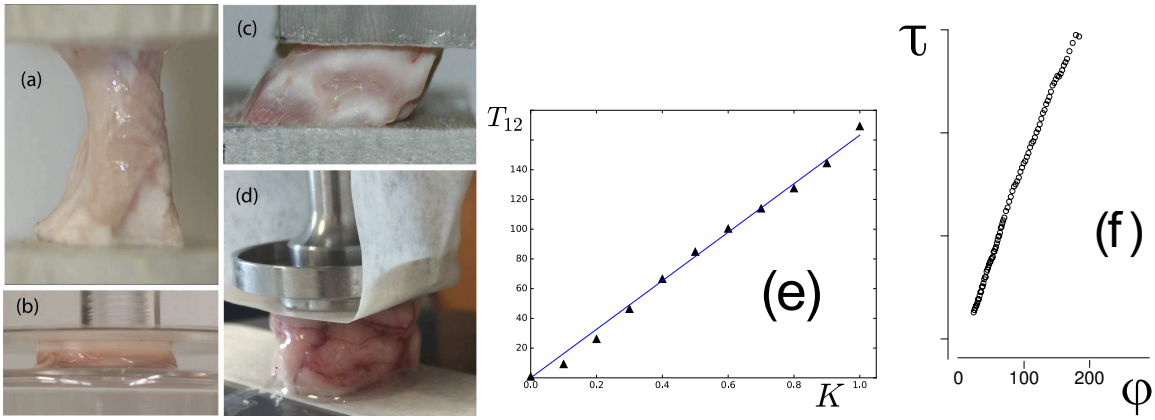

FIGURE 1. Standard testing protocols for soft solids applied to brain matter (porcine): (a) tensile test with glued ends and (b) compression test with lubricated faces: notice the inhomogeneity of the resulting deformations; (c) simple shear and (d) torsion: here the samples behave as required for the modelling. (e): shear stress Vs amount of shear [1]; (f): torque Vs twist [2].

where the λs are the principal stretches along the Eulerian principal directions x_1, x_2, x_3 (specifically, the body wave travels in the x_2-direction and is polarised in the x_1- direction).

Hence consider measuring the speed of a shear wave in an intact brain, subject to a small-but-finite compression described by $\lambda_1 = 1+e$, $\lambda_2 = \lambda_3 = 1-e/2+3e^2/8$, where e (small) is the amount of contraction (a contraction of 10% corresponds to $\lambda_1 = 0.9$, $e = -0.1$). Then the formula above gives [3],

$$\rho v^2 = \mu + (A/4)e + (2\mu + A + 3D)e^2, \tag{4}$$

where μ is the initial shear modulus, and A, D are the Landau coefficients of third- and fourth-order weakly non-linear elasticity, respectively. It is then a simple matter to estimate these material parameters, by collecting the $\rho v^2 - e$ data and fitting it to quadratic, see Figure 2.

With this talk we will explore further extensions of the theory of acousto-elasticity. First, with the propagation of waves in *thin-walled*, pre-stretched soft solids, which are commonly found in the body (Achille's tendon, arterial walls, bladder, mitral valve, dura matter, etc.). In that case the mathematics becomes more involved because of dispersion but good and practical approximations can be found. Then, with waves travelling on the surface of the human *skin*, which, it turns out, must be modelled as a pre-strained, hyperelastic solid with two orthogonal embedded families of parallel fibres [4].

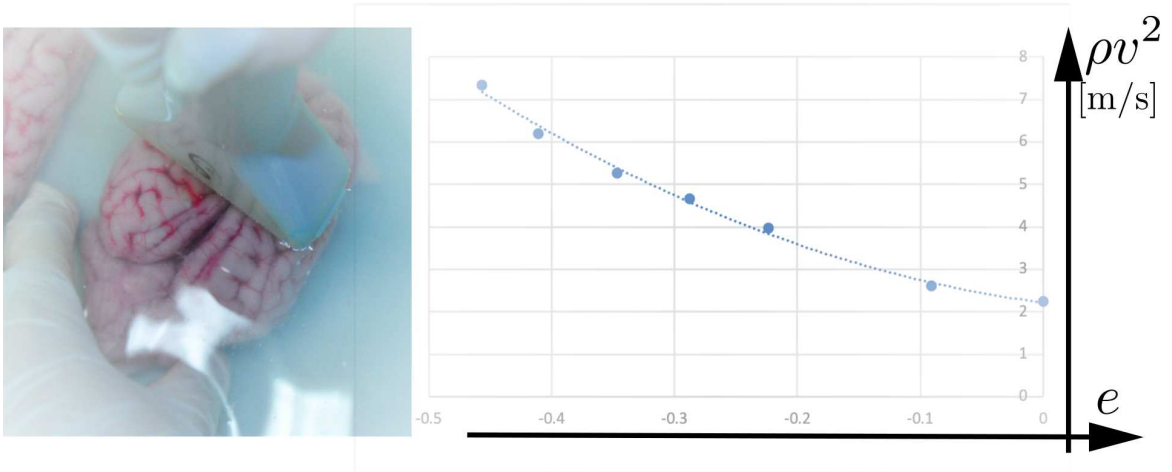

FIGURE 2. Using acousto-elasticity to find the material parameter of an intact pig brain. The curve fitting exercise on the right yields $\mu = 2.2$, $A = -15.0$, $D = 8.7$ kPa.

REFERENCES

[1] M. Destrade, M.D. Gilchrist, J.G. Murphy, B. Rashid, G. Saccomandi, *Extreme softness of brain matter in simple shear*, International Journal of Non-Linear Mechanics **75** (2015), 54–58.

[2] V. Balbi, A. Trotta, M. Destrade, A. Ní Annaidh, *Poynting effect of brain matter in torsion*, to appear.

[3] Y. Jiang, G. Li, L.X. Qian, S. Liang, M. Destrade, Y. Cao, *Measuring the linear and non-linear elastic properties of brain tissue with shear waves and inverse analysis*, Biomechanics and Modeling in Mechanobiology, 14(5) (2015), 1119–1128.

[4] C. Deroy, M. Destrade, A. Mc Alinden, A. Ní Annaidh, *Non-invasive evaluation of skin tension lines with elastic waves*, Skin Research and Technology **23**(3) (2017), 326–335.

PDE analysis of a class of thermodynamically compatible viscoelastic rate-type fluids with stress-diffusion

MIROSLAV BULÍČEK

SHORT ABSTRACT OF THE RESULT

Here we shortly describe the result of the presentation that was delivered in Oberwolfach during the workshop "Mathematical Aspects of Nonlinear Wave Propagation in Solid Mechanics" in March 4 - March 8, 2019. The result is published in [1].

Governing equation and the main result. For any given Lipschitz domain $\Omega \subset \mathbb{R}^d$, $d \geqslant 2$, $\boldsymbol{v}_0 : \Omega \to \mathbb{R}^d$, $b_0 : \Omega \to \mathbb{R}$ and for any $T > 0$, we set $Q := \Omega \times (0, T)$ and we seek the functions $(\boldsymbol{v}, p, b) : Q \to \mathbb{R}^d \times \mathbb{R} \times \mathbb{R}$ satisfying, in Q, the system

of PDEs:

$$\operatorname{div} \boldsymbol{v} = 0, \tag{1}$$

$$\varrho(\partial_t \boldsymbol{v} + \operatorname{div}(\boldsymbol{v} \otimes \boldsymbol{v})) - \operatorname{div} \mathbb{T} = 0, \tag{2}$$

$$\mathbb{T} = -p\,\mathbb{I} + 2\nu\mathbb{D} - \sigma(\nabla b \otimes \nabla b), \tag{3}$$

$$\nu_1 \partial_t b + \nu_1 \operatorname{div}(b\boldsymbol{v}) + \mu(b^2 - b) - 2\sigma b^2 \Delta b = 0, \tag{4}$$

together with the following boundary conditions, where $\boldsymbol{n}$ denotes the unit outward normal vector on $\partial\Omega$:

$$\boldsymbol{v} = \boldsymbol{0} \quad \text{and} \quad \nabla b \cdot \boldsymbol{n} = 0 \qquad \text{on } \partial\Omega \times (0,T), \tag{5}$$

and the initial conditions:

$$\boldsymbol{v}(0,\cdot) = \boldsymbol{v}_0(\cdot) \quad \text{and} \quad b(0,\cdot) = b_0(\cdot) \qquad \text{in } \Omega. \tag{6}$$

Here, $\boldsymbol{v}$ is the velocity, $\mathbb{T}$ is the Cauchy stress, p is the spherical stress (the modified pressure), b is a scalar quantity characterizing the volumetric elastic changes exhibited by the fluid; $\mathbb{D}$ denotes the symmetric part of the velocity gradient, i.e., $\mathbb{D} = (\nabla\boldsymbol{v} + (\nabla\boldsymbol{v})^{\mathrm{T}})/2$; ν is the viscosity, ϱ is the density, and ν_1, σ and μ are other material constants, all of which are positive.

The main result for the above system reads as

Theorem 1. *Let the initial conditions satisfy*

$$\begin{aligned} &\boldsymbol{v}_0 \in L^2_{0,\operatorname{div}}(\Omega)^d, \\ &b_0 \in W^{1,2}(\Omega), \quad b_0 > 0 \ \text{ a.e. in } \Omega, \quad b_0 \in L^\infty(\Omega) \quad \text{and} \quad \frac{1}{b_0} \in L^\infty(\Omega)\,, \end{aligned} \tag{7}$$

then for any Lipschitz domain $\Omega \subset \mathbb{R}^d$, $T > 0$, $\nu > 0$, $\nu_1 > 0$, $\mu > 0$, $\sigma > 0$ and $\varrho > 0$ there exists a couple $(\boldsymbol{v}, b)$ solving the problem (1)–(6) *in a weak sense.*

Derivation of the model and basic a priori estimates based on the first and the second laws of thermodynamics. Note that if $\sigma = 0$ in the above equations the problem splits into two separate problems: a transport equation with damping for b and the standard Navier–Stokes equations for $(\boldsymbol{v}, p)$. Since the work of Leray [4] on the incompressible Navier–Stokes equations, see also [3, 2], the question of long-time existence of large-data weak solutions has also been explored for more general classes of viscous fluids. It is then natural to attempt to advance this program by exploring how large the class of fluids might be for which long-time and large-data existence of weak solutions can be established. This task is particularly interesting if one considers fluid models that include terms that are associated with elastic properties of the material.

Note also that if $\sigma > 0$ then not only is there a diffusion term present in the equation for b, but also the Korteweg stress appears in the expression for the Cauchy stress $\mathbb{T}$ featuring in the equation for the balance of linear momentum. This structure of the governing equations results from a careful derivation of the model based on the thermodynamical approach established for viscoelastic rate-type fluids in [7] and further refined in [6], and extended to rate-type fluids with

stress-diffusion in [5]. This thermodynamical approach automatically guarantees that the resulting model is consistent with the laws of thermodynamics. From the point of view of PDE analysis, the approach readily provides the relevant *a priori* estimates upon which the analysis is based, and which would be otherwise completely nontrivial to discover solely from the PDE system (1)–(4).

We briefly explain the thermodynamical background of (1)–(4). We denote by the superscript $\dot{}$ the material derivative, i.e., $\dot{z} = \frac{\partial z}{\partial t} + (\boldsymbol{v}\cdot\nabla)z$ for a scalar function z. The fundamental balance equations of mass, linear momentum and energy as well as the formulation of the second law of thermodynamics are the following:

$$\dot{\varrho} = -\varrho \operatorname{div} \boldsymbol{v}, \tag{8}$$

$$\varrho\dot{\boldsymbol{v}} = \operatorname{div}\mathbb{T}, \qquad \mathbb{T} = \mathbb{T}^{\mathrm{T}}, \tag{9}$$

$$\varrho\dot{e} = \mathbb{T} : \mathbb{D} - \operatorname{div}\boldsymbol{j}_e, \tag{10}$$

$$\varrho\dot{\eta} = \varrho\zeta - \operatorname{div}\boldsymbol{j}_\eta \quad \text{with } \zeta \geqslant 0, \tag{11}$$

where ϱ is the density, $\boldsymbol{v}$ is the velocity, e is the specific internal energy, η is the specific entropy, $\boldsymbol{j}_e$ and $\boldsymbol{j}_\eta$ are the energy and entropy fluxes, and ζ stands for the specific rate of entropy production. Introducing the Helmholtz free energy ψ by

$$\psi := e - \theta\eta,$$

where θ stands for the (positive) temperature, the equations (10) and (11) lead for isothermal processes to

$$\mathbb{T} : \mathbb{D} - \varrho\dot{\psi} - \operatorname{div}(\boldsymbol{j}_e - \theta\boldsymbol{j}_\eta) = \xi \quad \text{with } \xi \geqslant 0, \tag{12}$$

where $\xi := \varrho\theta\zeta$ denotes the rate of dissipation.

The approach that we will exploit is based on the concept of natural configuration that splits the total response described by the deformation tensor $\mathbb{F}$ between the current and initial configuration into the purely elastic (reversible, non-dissipative) part $\mathbb{F}_{k_p(t)}$ that operates between the natural and current configuration and the dissipative part $\mathbb{G}$ that maps from the reference to the natural configuration, i.e. $\mathbb{F} = \mathbb{F}_{k_p(t)}\mathbb{G}$. In analogy with the relations $\mathbb{L} = \dot{\mathbb{F}}\mathbb{F}^{-1}$ and $\mathbb{D} = (\mathbb{L}+\mathbb{L}^{\mathrm{T}})/2$, we set $\mathbb{L}_{k_p(t)} := \dot{\mathbb{G}}\mathbb{G}^{-1}$ and define $\mathbb{D}_{k_p(t)} := (\mathbb{L}_{k_p(t)} + (\mathbb{L}_{k_p(t)})^{\mathrm{T}})/2$. We also set $\mathbb{B}_{k_p(t)} := \mathbb{F}_{k_p(t)}\mathbb{F}^{\mathrm{T}}_{k_p(t)}$. Finally, we postulate the constitutive relation for the Helmholtz free energy in the form:

$$\psi = \psi_0(\varrho) + \frac{\mu}{2\varrho}(\operatorname{tr}\mathbb{B}_{k_p(t)} - 3 - \ln\det\mathbb{B}_{k_p(t)}) + \frac{\sigma}{2\varrho}|\nabla \operatorname{tr}\mathbb{B}_{k_p(t)}|^2 =: \psi_0(\varrho) + \frac{\pi}{\varrho}, \tag{13}$$

with $\mu > 0$, $\sigma > 0$ constant, and

$$\pi := \frac{\mu}{2}(\operatorname{tr}\mathbb{B}_{k_p(t)} - 3 - \ln\det\mathbb{B}_{k_p(t)}) + \frac{\sigma}{2}|\nabla \operatorname{tr}\mathbb{B}_{k_p(t)}|^2.$$

Then after setting $b := \operatorname{tr}\mathbb{B}_{k_p(t)}$ and evaluating $\dot{\psi}$ in (12) we obtain (see [1] for details)

$$\begin{aligned}\xi = {} & \big(\mathbb{T} - \mu(\mathbb{B}_{k_p(t)} - \mathbb{I}) + \sigma((\nabla b \otimes \nabla b) + 2\Delta b\,\mathbb{B}_{k_p(t)}) + (\varrho^2\psi_0'(\varrho) - \pi)\mathbb{I}\big) : \mathbb{D} \\ & + \big(\mu(\mathbb{C}_{k_p(t)} - \mathbb{I}) - 2\sigma\Delta b\,\mathbb{C}_{k_p(t)}\big) : \mathbb{D}_{k_p(t)} - \operatorname{div}(\boldsymbol{j}_e - \theta\boldsymbol{j}_\eta + \sigma\dot{b}\,\nabla b) \quad \text{with } \xi \geqslant 0.\end{aligned}$$

Finally, setting

$$\boldsymbol{j}_\eta = \frac{\boldsymbol{j}_e + \sigma \dot{b}\, \nabla b}{\theta}, \qquad p_{\rm th}^{\rm NS} := \varrho^2\, \psi_0'(\varrho),$$
$$\mathbb{T}_{\rm el} := -(p_{\rm th}^{\rm NS} - \pi)\mathbb{I} + \mu(\mathbb{B}_{k_p(t)} - \mathbb{I}) - \sigma((\nabla b \otimes \nabla b) + 2\Delta b\, \mathbb{B}_{k_p(t)}),$$

we arrive at

$$\xi = (\mathbb{T} - \mathbb{T}_{\rm el}) : \mathbb{D} + \big(\mu(\mathbb{C}_{k_p(t)} - \mathbb{I}) - 2\sigma\Delta b\, \mathbb{C}_{k_p(t)}\big) : \mathbb{D}_{k_p(t)} \quad \text{with} \quad \xi \geqslant 0. \tag{14}$$

Reduction of the model. Here, we make three simplifications: the fluid is assumed to be incompressible, the density is taken to be uniform and the elastic part of the deformation is supposed to be purely spherical. This means that

$$\operatorname{div} \boldsymbol{v} = 0, \quad \varrho \text{ is a positive constant} \quad \text{and} \quad [\mathbb{C}_{k_p(t)}]_\delta = \mathbb{O}. \tag{15}$$

Then,

$$\mathbb{C}_{k_p(t)} = [\mathbb{C}_{k_p(t)}]_\delta + \frac{\operatorname{tr}\, \mathbb{C}_{k_p(t)}}{3}\mathbb{I} = \mathbb{O} + \frac{\operatorname{tr}\, \mathbb{B}_{k_p(t)}}{3}\, \mathbb{I} = \frac{b}{3}\, \mathbb{I},$$

where $\mathbb{O}$ is the zero tensor; note that $[\mathbb{B}_{k_p(t)}]_\delta$ also vanishes. As a consequence of these simplifications, we have

$$\dot{b} = -\frac{2}{3}\, b\, \operatorname{tr}\, \mathbb{D}_{k_p(t)}, \tag{16}$$

and

$$\xi = (\mathbb{T}_\delta - [\mathbb{T}_{\rm el}]_\delta) : \mathbb{D} + (\mu(b-3) - 2\sigma b\, \Delta b)\, \frac{\operatorname{tr}\, \mathbb{D}_{k_p(t)}}{3} \quad \text{with} \quad \xi \geqslant 0, \tag{17}$$

where

$$[\mathbb{T}_{\rm el}]_\delta = -\sigma(\nabla b \otimes \nabla b)_\delta.$$

Requiring that

$$\begin{aligned} \mathbb{T}_\delta - [\mathbb{T}_{\rm el}]_\delta &= 2\nu\, \mathbb{D} \qquad \text{with } \nu > 0, \\ \mu(b-3) - 2\sigma b\, \Delta b &= 2\nu_1 \frac{\operatorname{tr}\, \mathbb{D}_{k_p(t)}}{3} \qquad \text{with } \nu_1 > 0, \end{aligned} \tag{18}$$

we obtain

$$\xi = 2\nu|\mathbb{D}|^2 + 2\nu_1 \frac{|\operatorname{tr}\, \mathbb{D}_{k_p(t)}|^2}{9}. \tag{19}$$

Referring then to (16) we deduce that (18) leads to

$$\begin{aligned} \mathbb{T} &= m\mathbb{I} + 2\nu\mathbb{D} - \sigma(\nabla b \otimes \nabla b)_\delta = \phi\mathbb{I} + 2\nu\mathbb{D} - \sigma(\nabla b \otimes \nabla b), \\ \nu_1 \frac{\dot{b}}{b} &+ \mu(b-3) - 2\sigma b\, \Delta b = 0, \end{aligned} \tag{20}$$

which after a possible rescaling leads to (1)–(4).

References

[1] M. Bulíček, J. Málek, V. Průša, and E. Süli, *PDE analysis of a class of thermodynamically compatible viscoelastic rate-type fluids with stress-diffusion*, Mathematical analysis in fluid mechanics—selected recent results, Contemp. Math. **710** (2018), Amer. Math. Soc., Providence, RI, 25–51.

[2] L. Caffarelli, R. Kohn, and L. Nirenberg, *Partial regularity of suitable weak solutions of the Navier–Stokes equations*, Commun. Pure Appl. Math. **35** (1982), 771–831.

[3] E. Hopf, *Über die Anfangswertaufgabe für die hydrodynamischen Grundgleichungen*, Math. Nachr. **4** (1951), 213–231.

[4] J. Leray, *Sur le mouvement d'un liquide visqueux emplissant l'espace*, Acta Math. **63** (1934), 193–248.

[5] J. Málek, V. Průša, T. Skřivan, and E. Süli, *Thermodynamics of viscoelastic rate-type fluids with stress diffusion*, arXiv:1706.06277 (2017).

[6] J. Málek, K. R. Rajagopal, and K. Tůma, *On a variant of the Maxwell and Oldroyd-B models within the context of a thermodynamic basis*, Int. J. Non-Linear Mech. **76** (2015), 42–47.

[7] K.R. Rajagopal and A.R. Srinivasa, *A thermodynamic frame work for rate type fluid models*, Journal of Non-Newtonian Fluid Mechanics **88**(3) (2000), 207–227.

Viscoelasticitiy with limited strain: traveling waves and the Cauchy problem

Yasemin Şengül

The talk is concerned with the dynamics of a viscoelastic medium governed by the equation

$$T_{xx} + \nu T_{xxt} = g(T)_{tt}, \tag{1}$$

where $T(x,t)$ is the Cauchy stress at point x and time t, $g(T)$ is a nonlinear function and ν is a constant. Equation (1) is a one dimensional nonlinear differential equation in T resulting from the equation of motion and a constitutive equation relating the stress, the linearized strain and the strain rate. In the first part of the talk, I will investigate traveling wave solutions of (1) based on [4], whereas in the second part I will prove local well-posedness for the corresponding Cauchy problem based on [5].

As opposed to the classical models in mechanics, the strain can be written as a function of the stress, rather than expressing the stress in terms of the kinematical variables. As explained by Muliana et al. [7], force, and hence the stress, is the cause for deformation, hence for the strain. Because of this the strain should be described in terms of the stress or its history than vice versa. The motivation for this idea is that in the classical elasticity theory, there cannot be a nonlinear relationship between the linearized strain and the stress, which, in fact, is observed in some experiments. There are numerous models introduced by Rajagopal [10] with implicit constitutive relations between the stress and the strain including models for elastic fluids, inelastic materials and non-hyperelastic materials. Following these models, various forms of non-linear constitutive relations have been studied in different contexts (see e.g. [1, 2, 3, 11, 12]).

Rajagopal [8, 9, 10] introduced a generalization of the theory of elastic materials by suggesting implicit models allowing for approximations where the linearized strain is a nonlinear function of the stress. The advantage of this new idea is that it allows for the gradient of the displacement to stay small so that one could treat the linearized strain, even for arbitrary large values of the stress. The fracture of brittle elastic bodies is a possible application area for such implicit theories, where one can obtain bounded strain at the crack tip due to the possibility of having a nonlinear relationship between the linearized strain and the stress. There has been quite an interest in such strain-limiting models recently where most of the studies are for elastic materials. For the first part of the talk, I focus on five different nonlinear functions $g(T)$, that have been studied in the literature in the elastic setting, and reconsider them in the context of viscoelasticity. To describe the response of viscoelastic solids I assume a nonlinear relationship among the linearized strain, the strain rate and the Cauchy stress. I look at traveling wave solutions that correspond to the heteroclinic connections between the two constant states, and establish conditions for the existence of such solutions, and find them explicitly, implicitly or numerically.

In the second part of the talk, I am interested in local well-posedness of equation (1). For viscoelasticity, not much has been done in the literature. One can refer to Muliana et al. [7] who developed a quasi-linear viscoelastic model where the strain is expressed as an integral of a non-linear measure of the stress, or to Rajagopal and Saccomandi [12] where rate-type strain-limiting viscoelasticity is modelled by considering a special subclass of the general implicit constitutive relations. In [5] we convert the equation for the stress to obtain an equation in the strain variable and write it as a time-dependent heat equation. We use the results related to the variable coefficient heat equation and the techniques from the theory of elliptic operators. The proof of the main theorem includes linearization around a given state, definition of a contractive mapping and the usage of Banach's fixed theorem.

References

[1] M. Bulíček, J. Málek, K.R. Rajagopal, E. Süli, *On elastic solids with limiting small strain: modelling and analysis*, EMS Surv. Math. Sci. **1**(2) (2014), 283–332.

[2] R. Bustamante, *Some topics on a new class of elastic bodies*, Proc. R. Soc. A **465** (2009), 1377–1392.

[3] R. Bustamante, K.R. Rajagopal, *Solutions of some simple boundary value problems within the context of a new class of elastic materials*, Int. J. Nonlinear Mech. **46**(2) (2011), 376–386.

[4] H.A. Erbay, Y. Şengül, *Traveling waves in one-dimensional non-linear models of strain-limiting viscoelasticity*, Int. J. Non-Linear Mech. **77** (2015), 61–68.

[5] H.A. Erbay, A. Erkip and Y. Şengül, *Local existence of solutions to the initial-value problem for one-dimensional strain-limiting viscoelasticity*, preprint.

[6] K. Kannan, K.R. Rajagopal, G. Saccomandi, *Unsteady motions of a new class of elastic solids*, Wave Motion **51** (2014), 833–843.

[7] A. Muliana, K.R. Rajagopal, A.S. Wineman, *A new class of quasi-linear models for describing the nonlinear viscoelastic response of materials*, Acta Mech. **224** (2013), 2169–2183.

[8] K.R. Rajagopal, *On implicit constitutive theories*, Appl. Math. **48** (2003), 279–319.

[9] K.R. Rajagopal, *The elasticity of elasticity*, Z. Angew. Math. Phys. **58** (2007), 309–317.

[10] K.R. Rajagopal, *On a new class of models in elasticity*, J. Math. Comput. Appl. **15** (2010), 506–528.
[11] K.R. Rajagopal, *On the nonlinear elastic response of bodies in the small strain range*, Acta. Mech. **225** (2014), 1545–1553.
[12] K.R. Rajagopal, G. Saccomandi, *Circularly polarized wave propagation in a class of bodies defined by a new class of implicit constitutive relations*, Z. Angew. Math. Phys. **65** (2014), 1003–1010.

One-dimensional nonlinear waves in nonlocal elastic materials

Husnu Ata Erbay
(joint work with S. Erbay, A. Erkip)

In contrast with classical elasticity, the theory of nonlocal elasticity is based on integral constitutive relations in which the stress at a point depends on the strain field at every point in the body [1]. There is a large literature concerning the theory of nonlocal elasticity but they are mostly restricted to linear models of nonlocal elasticity. In [2] a one-dimensional nonlinear model of nonlocal elasticity was proposed and, under certain conditions, the global existence of solutions to the initial-value problem was established. In terms of non-dimensional quantities, the model in [2] is based on the one-dimensional nonlinear nonlocal partial differential equation

$$u_{tt} = (\beta * (u + g(u)))_{xx} \tag{1}$$

with

$$\beta * u = \int_{\mathbb{R}} \beta(x-y)u(y)dy,$$

where β is an integrable function whose Fourier transform is nonnegative. Some well-known examples of nonlinear wave equations, such as Boussinesq-type equations, follow from the above model for suitable choices of the kernel function β. For instance, when $\beta(x) = e^{-|x|}/2$, equation (1) becomes the improved Boussinesq equation

$$u_{tt} - u_{xx} - u_{xxtt} = (g(u))_{xx}. \tag{2}$$

In this talk we review some recent results concerning the nonlocal model given above. *(i)* We start with a convergence result for a semi-discrete numerical method proposed for the Cauchy problem and, as an application of this result, in the case of several kernel functions we compute numerically the blow-up times for solutions that blow-up in a finite time [3]. *(ii)* Next we present a comparison result for the solutions of the two Cauchy problems with the same initial data but with two different kernel functions that have similar dispersive characteristics in the long-wave limit. The comparison result shows that the difference between the two solutions remains small over a long time interval in a suitable Sobolev norm [4]. *(iii)* Finally we discuss the approximation errors for Camassa-Holm-type asymptotical models describing the propagation of small-but-finite amplitude long

waves as solutions to the nonlocal equation. A careful theoretical analysis allows us to justify the single Camassa-Holm equation

$$w_t + w_x + ww_x - \frac{3}{4}w_{xxx} - \frac{5}{4}w_{xxt} - \frac{3}{4}(2w_xw_{xx} + ww_{xxx}) = 0 \tag{3}$$

for the unidirectional propagation of waves [5]. In order to write (3) in a more standard form we may use the coordinate transformation defined by $\bar{x} = \frac{2}{\sqrt{5}}(x - \frac{3}{5}t)$ and $\bar{t} = \frac{2}{3\sqrt{5}}t$. Under the coordinate transformation, (3) becomes

$$v_{\bar{t}} + \frac{6}{5}v_{\bar{x}} + 3vv_{\bar{x}} - v_{\bar{t}\bar{x}\bar{x}} - \frac{9}{5}(2v_{\bar{x}}v_{\bar{x}\bar{x}} + vv_{\bar{x}\bar{x}\bar{x}}) = 0, \tag{4}$$

with $v(\bar{x}, \bar{t}) = w(x, t)$. A similar analysis based on the two uncoupled Camassa-Holm equations is also shown to be valid for bidirectional wave solutions of the improved Boussinesq equation [6]. We show that, in both cases, the approximation errors remain small in terms of nonlinearity and dispersion parameters over a long time interval.

References

[1] A.C. Eringen, *Nonlocal Continuum Field Theories*, Springer, New York, 2002.

[2] N. Duruk, H.A. Erbay, A. Erkip, *Global existence and blow-up for a class of nonlocal nonlinear Cauchy problems arising in elasticity*, Nonlinearity, **23** (2010), 107–118.

[3] H.A. Erbay, S. Erbay, A. Erkip, *Convergence of a semi-discrete numerical method for a class of nonlocal nonlinear wave equations*, ESAIM: Math. Model. Numer. Anal., **52** (2018), 803–826.

[4] H.A. Erbay, S. Erbay, A. Erkip, *Comparison of nonlocal nonlinear wave equations in the long-wave limit*, Applicable Analysis, https://doi.org/10.1080/00036811.2019.1577393.

[5] H.A. Erbay, S. Erbay, A. Erkip, *The Camassa-Holm equation as the long-wave limit of the improved Boussinesq equation and of a class of nonlocal wave equations*, Discrete Contin Dyn Syst., **36** (2016), 6101–6116.

[6] H.A. Erbay, S. Erbay, A. Erkip, *On the decoupling of the improved Boussinesq equation into two uncoupled Camassa-Holm equations*, Discrete Contin Dyn Syst. **37** (2017), 3111–3122.

Lipschitz metrics for nonlinear PDEs

Katrin Grunert

(joint work with J. A. Carrillo, H. Holden)

Partial differential equations, that govern the motion of waves, model also wave phenomena such as wave breaking. One example of such an equation is the Hunter–Saxton equation

$$u_t(t,x) + uu_x(t,x) = \frac{1}{4}\int_{-\infty}^{x} u_x^2(t,y)dy - \frac{1}{4}\int_{x}^{\infty} u_x^2(t,y)dy,$$

which we will consider here. It models the director field of a nematic liquid crystal [7].

Starting out with some smooth initial data, one obtains, in general, no classical global solution. To be more precise, classical solutions do not exist globally, but only locally in time, if wave breaking occurs in finite time. That is, the spatial derivative u_x becomes unbounded from below pointwise, while the solution u itself remains bounded and continuous. Furthermore, energy concentrates on sets of measure zero when wave breaking occurs. Thus the prolongation of solutions beyond wave breaking is non-unique and depends heavily on how the concentrated energy is manipulated.

In this talk we motivate how to construct a Lipschitz metric, which measures the distance between two conservative solutions, i.e., solutions where the energy is not manipulated at breaking time. Such metrics show in what sense the solutions are stable and reflect the influence of the wave phenomena on the solutions. We focus on the approach used in [4] and compare it with the approach used in [8].

The approach in [8] relies on the fact that conservative solutions of the Hunter–Saxton equation can be described with the help of a generalized method of characteristics. Thus one way to measure the distance between two solutions, is to define their distance to be equal to the distance of the corresponding equivalence classes in Lagrangian coordinates. The drawback of this idea is that it is very difficult to compute the difference even for very simple examples.

The approach in [4] is based on the fact that each solution is uniquely determined by a pair (u, μ), where μ describes the energy distribution. In the case of the total energy being equal to one, μ can be seen as a probability measures, for which a natural way to measure the distance are Wasserstein metrics. With this observation in mind, one can use pseudo inverses together with relabeling to introduce new variables, which form the basis for our approach. These new variables have the good properties of the Lagrangian coordinates, but not the extra degree of freedom leading to equivalence classes.

Similar results can be obtained for the Camassa–Holm equation, see [6] and [5], respectively.

References

[1] A. Bressan, H. Holden, X. Raynaud, *Lipschitz metric for the Hunter–Saxton equation*, J. Math. Pures. Appl. **94** (2010), 68–92.

[2] A. Bressan, P. Zhang, Y. Zheng, *Asymptotic variational wave equations*, Arch. Ration. Mech. Anal. **183** (2007), 163–185.

[3] J. A. Carrillo, M. Di Francesco, C. Lattanzio, *Contractivity of Wasserstein metrics and asymptotic profiles for scalar conservation laws*, J. Differential Equations **231** (2006), 425–458.

[4] J. A. Carrillo, K. Grunert, H. Holden. *A Lipschitz metric for the Hunter–Saxton equation*, Comm. Part. Diff. Eqs. (to appear).

[5] J.A. Carrillo, K. Grunert, H. Holden. *Lipschitz metrics for the Camassa–Holm equation*, available soon on arXiv.

[6] K. Grunert, H. Holden, X. Raynaud. *Lipschitz metric for the Camassa–Holm equation on the line*, Discrete Cont. Dyn. Syst. **33** (2013), 2809–2827.

[7] J- K. Hunter, R. Saxton. *Dynamics of director fields*, SIAM J. Appl. Math. **51** (1991), 1498–1521.
[8] A. Nordli. *A Lipschitz metric for conservative solutions of the two-component Hunter-Saxton system*, Methods Appl. Anal. **23** (2016), 215–232.

Shear shock wave propagation in soft solids and the brain: ultrasound imaging and simulations

Gianmarco Pinton

The soft tissue of the human body supports both fast acoustic waves (1540 m/s) and slow shear waves (2 m/s). At large amplitudes, these waves exhibit nonlinear behavior, such as harmonic development and shock formation. We develop models and simulation tools that describe the physics of nonlinear acoustic propagation, attenuation, and scattering in highly realistic representations of the human body. We use these models to develop new ultrasound imaging methods. For example, to understand brain motion during the rapid events associated with traumatic injury, we have developed a new high framerate (10,000 images/second) imaging technique that measures image brain motion down to the micron level. By interrogating this spatiotemporal regime, we have discovered that destructive shear shock waves form and propagate deep inside the brain. We develop models and simulation tools that describe the formation, propagation, and attenuation of these shock waves in the brain. It is shown experimentally and numerically that this previously unknown phenomenon can dramatically amplify the acceleration and strain rates within the brain.

Riemann-Cartan geometry as a framework for modeling of nonlinear dispersive waves in solids

Ilya Peshkov

We are developing a unified Riemann-Cartan theory for continuum solid and fluid mechanics. The continuous medium is treated as a Riemann-Cartan manifold with the main field of the theory being the field of anholonomic basis triads, also called the distortion field in our papers. The distortion field describes micro-deformations and micro-rotations of the material elements. To account for the rotational degrees of freedom, we use the torsion tensor and treat it as a new independent state variable. We observed that the obtained system of governing PDEs can be viewed as a non-classical dispersive system in which all the equations are first order PDEs while the dispersive terms are local relaxation-type source terms. We then discuss possible applications of the theory to the modeling of dispersive waves in acoustic metamaterials.

The mechanics of a twisted brain

Valentina Balbi

Biological soft tissues are particularly common in nature. For instance, many organs in the human body such as the skin, the brain, the gastro-intestinal system are made of soft tissues. The brain, among all is particularly soft and delicate. Following an impact to the skull, brain matter can experience large stretches, possibly resulting in Diffuse Axonal Injury (DAI), which is the second leading cause of death from traumatic brain injury in the United States [1]. Previous

Figure 1. A boxer receiveing a lateral punch which induces an accelerated rotation of the head.

studies have focused on tensile, compression and shear deformation modes of brain to investigate DAI. A comprehensive collection of mechanical data (elastic and viscoelastic) can be found in [2]. However, in reality brain matter undergoes a mix of deformation modes during an accident. Especially during sport and car accidents the head may be subjected to a quick rotation which in turn generates twisting moments within the brain tissue, see Figure 1. Therefore modelling the mechanical behaviour of the tissue in torsion is crucial to help gaining a better understanding of the mechanisms of DAI.

In this work, in collaboration with University College Dublin, we collected data from torsion tests on (pigs) brain samples and modelled the experiments to finally quantify the elastic properties of the brain tissue. By using a rheometer (Discovery HR-2, TA instruments®), we tested 9 cylindrical samples and measured the torque and the normal force required to twist each sample at a constant twist rate (a measure of the rotational speed). From our experiments we observed that the brain pushes against the upper plate of the rheometer when twisted (see Figure 2), indicating that the tissue tends to expand in the direction perpendicular to the twisting plane, a typical effect which is called the positive Poynting Effect [3]. By using the theory of non linear elasticity we followed Rivlin [4] and derived the equations for the torque and the normal force and we fitted the experimental data with a Mooney-Rivlin (MR) strain energy function. With this procedure we were able to extract the two elastic constants appearing in the MR model and thus quantify the shear modulus of the brain and the Poyniting effect (given by the second MR constant). We then used the elastic parameters to implement Finite Element (FE) simulations of a rotational head impact in Abaqus. In Figure

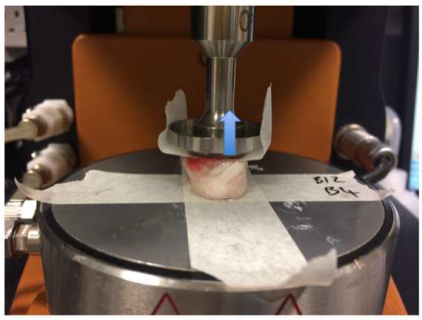

FIGURE 2. The brain tends to expand longitudinally when twisted.

3 we show the distribution of the normal and shear Cauchy stress components S_{33} and S_{23}, respectively, in the brain. These results were obtained with the University College Dublin Brain Trauma Model (UCDBTM) [5]. To simulate a realistic impact scenario we used the rotational acceleration values measured from studies on boxing accidents. The simulations show that during such impacts the brain experiences not only high shear stresses, but also high normal stresses. We then concluded that it is crucial to account for the normal forces developing within the brain during rotational impacts to correctly estimate the effects of TBI.

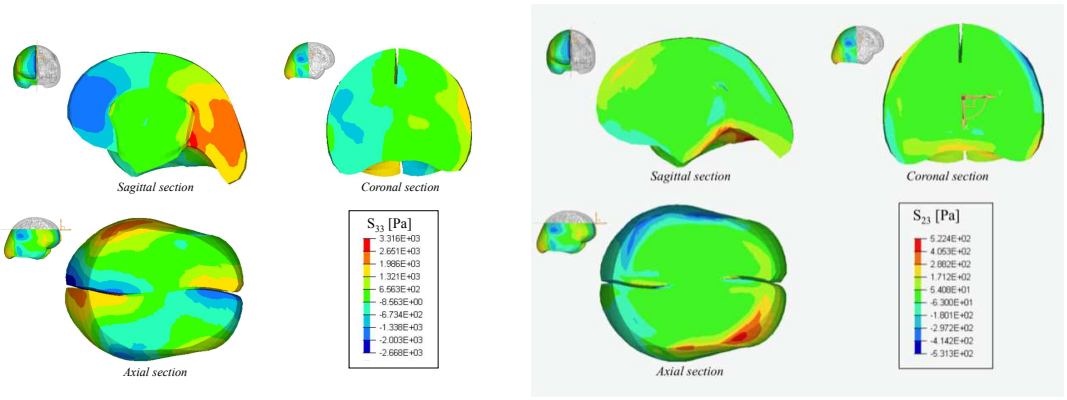

FIGURE 3. FE simulation of a rotational head impact. Distribution of the normal (left) and shear (right) Cauchy stress components within the brain.

REFERENCES

[1] C.A. Taylor, J.M. Bell, M.J. Breiding, L. Xu, *Traumatic Brain Injury-Related Emergency Department Visits, Hospitalizations, and Deaths-United States, 2007 and 2013*, Morbidity and mortality weekly report Surveillance summaries (Washington, DC: 2002) **66**(9) (2017), 1–16.

[2] S. Chatelin, A. Constantinesco, R. Willinger, *Fifty years of brain tissue mechanical testing: from in vitro to in vivo investigations*, Biorheology **47**(5-6) (2010), 255–276.

[3] J.H. Poynting, *On pressure perpendicular to the shear planes in finite pure shears, and on the lengthening of loaded wires when twisted*, Proceedings of the Royal Society of London Series A, Containing Papers of a Mathematical and Physical Character **82**(557) (1909), 546–559.
[4] R.S. Rivlin, D. Saunders, *Large elastic deformations of isotropic materials VII. Experiments on the deformation of rubber*, Philosophical Transactions of the Royal Society of London Series A, Mathematical and Physical Sciences **243**(865) (1951), 251–288.
[5] T.J. Horgan, M.D. Gilchrist, *The creation of three-dimensional finite element models for simulating head impact biomechanics*, International Journal of Crashworthiness **8**(4) (2003), 353–366.

Shear wave pattern in the elastodynamic of a cracked half-space with microstructure

Andrea Nobili
(joint work with Enrico Radi, Gennadi Mishuris)

We investigate diffraction of reduced traction shear waves applied at the faces of a stationary crack in an elastic solid with microstructure, under antiplane deformation. The material behavior is described by the indeterminate theory of couple stress elasticity and the crack is rectilinear and semi-infinite. A remarkable wave pattern appears which consists of entrained waves extending away from the crack, reflected Rayleigh waves moving along the crack, localized waves irradiating from the crack-tip with, possibly, super-Rayleigh speed and body waves scattered around the crack-tip. The displacement along the crack line is given by [3]

$$w(\xi_1,0,\tau)=\imath\lambda^3\tau_0\frac{\exp\imath\Omega\tau}{\pi K^-(k)}\int_{\mathscr{L}}\frac{\exp(-\imath s\xi_1)}{(s+k)K^-(s)}\mathrm{d}s,$$

where (c is a constant, a is the Rayleigh pole and b the leaky pole)

$$K^{\pm}(s)=\sqrt{c}\frac{(s\mp a)(s\pm\imath b)}{\alpha^{\pm}(s)}\frac{s\pm s_3}{s\pm s_0}F^{\pm}(s).$$

Here

$$\alpha^{\pm}(s)=e^{\mp\imath\pi/4}\sqrt{s\mp\delta},\quad \beta^{\pm}(s)=e^{\mp\imath\pi/4}\sqrt{s\pm\imath},$$

with $F^{\mp}(s)=\exp G^{\mp}(s)$, being

$$G^-(s)=\frac{\delta+\imath}{\pi}\int_0^1\frac{\arctan\psi(t)}{\delta-(\delta+\imath)t+s}\mathrm{d}t,$$

and

$$\psi(t)=\left(\frac{(1+\eta)[(\delta+\imath)t-\delta]^2-\delta^2}{(1+\eta)[(\delta+\imath)t-\delta]^2+1}\right)^2\sqrt{\frac{(1-t)^2\delta-\imath(1-t^2)}{(2-t)\delta t-\imath t^2}}.$$

Ahead of the crack tip, displacement can be conveniently determined closing the integration path $\mathscr{L}$ around the top branch cut, $\mathcal{K}^+$, and adding the contribution

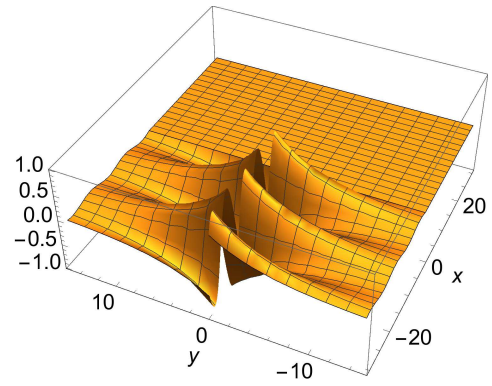

(A) Displacement wave entrained by the traction shear wave applied at the crack faces

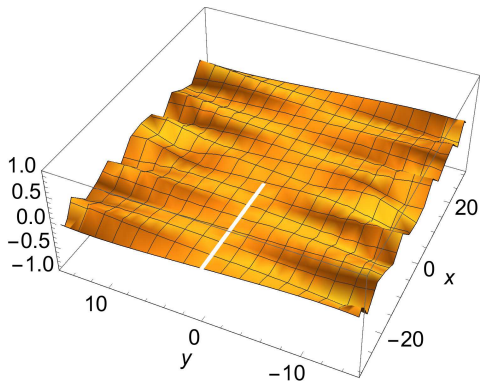

(B) Scattered body wave

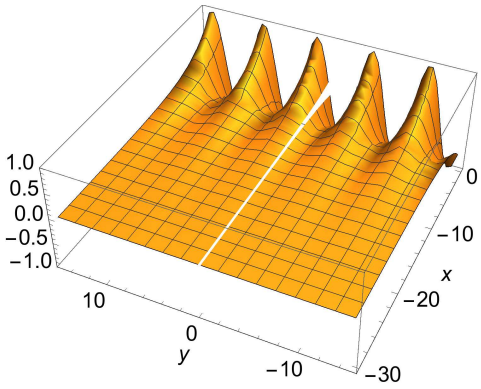

(C) Localized wave travelling along ξ_2

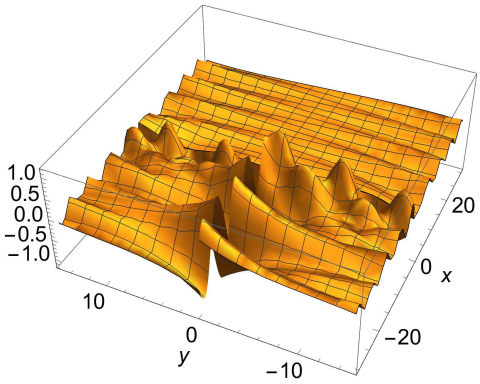

(D) Total wave pattern

FIGURE 1. Schematic representation of the wave pattern for $k < -a$ (each wave is scaled as to improve clarity and only one wave is considered for each contribution; reflected Rayleigh waves are disregarded)

of the poles $s = -k, -a$ and $s = \imath b$, namely

$$w(\xi_1, 0, \tau) = -2\lambda^3 \tau_0 \frac{\exp \imath\Omega\tau}{K^-(k)} \left[\frac{1}{2\pi\imath} \int_{\mathcal{K}^+} \frac{\exp(-\imath s\xi_1)}{(s+k)K^-(s)} \mathrm{d}s + \frac{\exp(\imath k\xi_1)}{K^+(k)} \right.$$
$$\left. - \frac{\exp(\imath a\xi_1)}{k-a} \frac{\alpha^+(a)}{\sqrt{c}(a+\imath b)F^+(a)} \frac{a+s_0}{a+s_3} + \frac{\exp(b\xi_1)}{k+\imath b} \frac{\alpha^-(\imath b)}{\sqrt{c}(a+\imath b)F^-(\imath b)} \frac{\imath b - s_0}{\imath b - s_3} \right], \quad \xi_1 < 0.$$

We remark that simple poles represent travelling waves. Indeed, the second term in square brackets provides the displacement wave entrained by the traction wave applied at the crack faces, Fig.1a, while the third term brings *outgoing* Rayleigh waves, reflected by the crack-tip. The last term is remarkable in that it represents waves that decay exponentially for $\xi_1 < 0$ and yet propagate along the ξ_2 direction,

Fig.1c. To see this, we note that $\alpha(\imath b) = -\imath\sqrt{b^2+\delta^2}$ and $\beta(\imath b) = -\imath\sqrt{b^2-1}$, whence a pair of waves arises with speed

$$\frac{c_{b1}}{c_s} = \frac{\Omega}{\sqrt{b^2+\delta^2}}\lambda, \quad \text{and} \quad \frac{c_{b2}}{c_s} = \frac{\Omega}{\sqrt{b^2-1}}\lambda.$$

Such waves may be put to great advantage in non-destructive material testing for they are highly localized along ξ_1 in correspondence of the crack-tip location. Furthermore, we observe that unlike $c_{b1} < c_R \leq c_s$, c_{b2} may be very large and greater than the Rayleigh wave speed. The possibility of surface waves moving at super-Rayleigh speed in couple-stress materials has been pointed out in [2] and discussed in [4, 1], in the context of plane strain. Interestingly, we note that for $\eta = 0$, $s = -a$ and $s = \imath b$ are no longer poles. The first term in square brackets represents non-planar body waves, moving with speed $\tilde{c}$ along the crack line and away from the crack-tip, Fig.1b.

It's interesting to observe that unboundedness (resonance) occurs only for $k = -a$, that is when the reduced traction shear wave is associated with Rayleigh edge-waves being fed *into* the crack-tip. Indeed, when $k = a$ and Rayleigh waves move *out* of the crack-tip, the second and the third term in square brackets combine into a bounded term.

We now consider the pole $s = -k$ in the context of the full-field solution. Then, the real interval $|k| < \delta$ is associated with a decaying and a propagating wave along ξ_2, the latter with speed $c \geq c_R$ greater than Rayleigh. Indeed, this result corresponds to a super-Rayleigh loading condition. The condition of exponential loading, $k = \imath k_2, -1 < k_2 < 0$, still brings a pair of waves along ξ_2, one decaying and the other propagating, yet the latter moves with sub-Rayleigh speed $\Omega\lambda c_s(k_2^2+\delta^2)^{-1/2}$. However, when decay is strong enough along ξ_1, i.e. $k_2 < -1$, the decaying wave turns propagating along ξ_2 with speed $\Omega\lambda c_s/\sqrt{k_2^2-1}$, which generally exceeds c_R.

By Jordan's lemma [5, §1.5], the displacement $w(\xi_1, 0)$ vanishes beyond the crack tip, in agreement with the boundary conditions. The full displacement field beyond the crack-tip is obtained closing the integration path around $\mathcal{K}^-$. Then, only body waves moving with speed $\tilde{c}$ along the crack line and away from the crack-tip appear. It is concluded that the crack tip acts as a scatterer of the applied traction shear wave, Fig.1d.

References

[1] H.G. Georgiadis, E.G. Velgaki, *High-frequency Rayleigh waves in materials with micro-structure and couple-stress effects*, International Journal of Solids and Structures, **40**(10) (2003):2501–2520.

[2] K.F. Graff, Y.H. Pao, *The effects of couple-stresses on the propagation and reflection of plane waves in an elastic half-space*, Journal of Sound and Vibration, **6**(2) (1967):217–229.

[3] A. Nobili, E. Radi, A. Vellender, *Diffraction of antiplane shear waves and stress concentration in a cracked couple stress elastic material with micro inertia*, Journal of the Mechanics and Physics of Solids, **124** (2019): 663–680.

[4] N.S. Ottosen, M. Ristinmaa, C. Ljung, *Rayleigh waves obtained by the indeterminate couple-stress theory*, European Journal of Mechanics-A/Solids, **19**(6) (2000):929–947.
[5] B.W. Roos. *Analytic functions and distributions in physics and engineering*, John Wiley and Sons, Inc., New York (USA), 1969.

Traveling and standing solitary waves in a prestressed coated elastic half-space.

Yibin Fu

The current study is motivated by the recent surge of interest in strain-induced buckling patterns that are recognized to have applications at the micrometer and submicrometer scales ranging from cell patterning, optical gratings, and creation of surfaces with desired wetting and adhesion properties, to metrology of ultrathin film properties. One of the fundamental problems that has been much studied is the buckling of a compressed coated half-space. It is known that when the coating is much stiffer than the half-space, the initial sinusoidal buckling pattern may in general suffer a period-doubling secondary bifurcation [1, 2]. However, if the substrate is subjected to a large enough prestretch before the coated half-space is compressed, then the period-doubling wrinkling pattern is replaced by a mountain ridge pattern that looks like a standing solitary wave ([3], figure 14). We first compute traveling solitary wave solutions for a coated elastic half-space that is subjected to a general uniaxial compression. We then increase the compression to reduce the wave speed to zero in order to obtain standing solitary wave solutions. Connections will be made with previous studies of solitary waves in coated half-spaces that are un-stressed [4, 5, 6].

References

[1] F. Brau, H. Vandeparre, A. Sabbah, C. Poulard, A. Boudaoud, P. Damman, *Multiple-length-scale elastic instability mimics parametric resonance of nonlinear oscillators*, Nat. Phys. **7** (2011), 56–60.
[2] Y.B. Fu, Z.X. Cai, *An asymptotic analysis of the period-doubling secondary bifurcation in a film/substrate bilayer*, SIAM J. Appl. Math. **75** (2015), 2381–2395.
[3] Y.P. Cao, J.W. Hutchinson, *Wrinkling phenomena in neo-Hookean film/substrate bilayers*, ASME J. Appl. Mech. **79** (2012), 031019.
[4] A. Porubov, A. M. Samsonov, *Long non-linear strain waves in layered elastic half-space*, Int. J. Non-linear Mechanics **30** (1995), 861–877.
[5] C. Eckl, A.P. Mayer, A.S. Kovalev, *Do surface acoustic solitons exist?*, Phys. Rev. Lett. **81** (1998), 983–986.
[6] A.S. Kovalev, A.P. Mayer, C. Eckl, G.A. Maugin, *Solitary Rayleigh waves in the presence of surface nonlinearities*, Phy. Rev. E **66** (2002), 036615.

Large strain viscoelastic response of fibre-reinforced materials

Jacopo Ciambella

Fibre-reinforced solids are a class of materials ubiquitously found either in nature and in artificially made structures. They have peculiar mechanical characteristics that derive from the combination of a (soft) homogeneous matrix with (stiff) reinforcing fibres [1]. Examples includes muscles, arteries, elastomers and soft gels, to cite but a few. Despite being macroscopically diverse, these materials share microstructural similarities due to the presence of long-chain molecules intertwined to each other, which form a spaghetti-like bundled structure with a high-degree of flexibility. As a result of an externally imposed stress, the long chains may alter their configurations relatively rapidly due to their high mobility. The requirement of linking the chains into a network structure is associated with solid-like features, which allow the material to be stretched up to about ten times of its original length. In addition, the long molecules may partially slide onto each other causing an internal reorganization which, macroscopically, manifests itself in a viscous-like behaviour. The combination of these two effects allows the materials to exhibit simultaneously the characteristics of a viscous fluid and of an elastic solid.

Reliable constitutive equations, able to predict correctly these effects and energy dissipation at finite strains, must consider the dependence of the stress upon the entire strain history (materials with memory). To date, several modelling strategies have been proposed, including: state variables [2], hereditary integral [3] and multi-integral formulations [4], as well as elastic-viscoplastic constitutive relationships [5].

In this talk, I will present a microscopically informed model to describe the large strain viscoelastic response of fibre-reinforced solids. The main kinematic assumption consists in the multiplicative decomposition of the deformation gradient into a viscous and an elastic part:

$$\mathbf{F} = \mathbf{F}_v \mathbf{F}_e \tag{1}$$

in which $\mathbf{F}_e$ is the macroscopic degree of freedom associated with the elastic (reversible) deformation, whereas $\mathbf{F}_v$ is the microscopic degree of freedom associated with the material reorganisation (irreversible process). In addition, at each material point x in the current configuration of the solid, one can define the local orientation of the microstructure through the unit vector field $\mathbf{n}$.

If we further assume that dissipation only occurs because of the internal reorganization of the long molecular chains, the elastic strain energy must depend on the elastic part of the deformation gradient through the left-Cauchy Green strain tensor, i.e., $\boldsymbol{B}_e = \mathbf{F}_e \mathbf{F}_e^T$. With this in hand, the internal rate of working is

$$\begin{aligned} \mathcal{W}^{int} = \dot{\mathcal{F}} &= \int_{\mathcal{P}_t} \frac{1}{2}(\rho \boldsymbol{v}^2)^{\cdot} + \rho \dot{\Psi}(\boldsymbol{B}_e, \boldsymbol{n} \otimes \boldsymbol{n}) \\ &= \int_{\mathcal{P}_t} \big(\rho \dot{\boldsymbol{v}} \cdot \boldsymbol{v} + \rho \frac{\partial \Psi}{\partial \boldsymbol{B}_e} \cdot \dot{\boldsymbol{B}}_e + \rho \frac{\partial \Psi}{\partial \boldsymbol{A}} \cdot \dot{\boldsymbol{A}}\big) \mathrm{d}v \end{aligned} \tag{2}$$

in which the structural tensor $\mathbf{A} = \mathbf{n} \otimes \mathbf{n}$ appears in strain energy density due to the transverse isotropy nature of the material. As such, the external rate of working is given by

$$\mathcal{W}^{ext} = \int_{\mathcal{P}_t} \boldsymbol{b} \cdot \boldsymbol{v} \, \mathrm{d}v + \int_{\partial\mathcal{P}_t} \boldsymbol{t} \cdot \boldsymbol{v} \, \mathrm{d}a + \int_{\mathcal{P}_t} \boldsymbol{g} \cdot \dot{\boldsymbol{n}} \, \mathrm{d}v + \int_{\mathcal{P}_t} \boldsymbol{\sigma}_v \cdot \boldsymbol{B}_e^{\triangledown} \, \mathrm{d}v \tag{3}$$

where $\boldsymbol{b}$ and $\boldsymbol{t}$ are the external body force and surface traction, respectively, and $\boldsymbol{b}$ is the velocity field. $\boldsymbol{g}$ are the external generalised forces conjugate to the microstructure and represent an *external body moment*. In Eq. (3) $\boldsymbol{\sigma}_v$ is the so called *active stress*, that is the dual variable of the internal remodelling velocity $\boldsymbol{B}_e^{\triangledown} = \mathbf{F}\big(\mathbf{F}_v^{-1}\mathbf{F}_v^{-T}\big)^{\cdot}\mathbf{F}^T$ also known as *Oldroyd upper convected derivative* [6]. By prescribing that the dissipation must be positive for every realizable process, one obtain the Clausius-Duhem inequality, which prescribes a positive dissipation for every realizable process:

$$\mathcal{D} = \mathcal{W}_{ext} - \mathcal{W}_{int} = \int_{\mathcal{P}_t} \xi \, \mathrm{d}v, \qquad \xi \geq 0. \tag{4}$$

On substituting (2) and (3) in (4) and on assuming that the material response is *elastic* with respect to the natural configuration and dissipation is only associated to the *microscopic reorganization*, one obtains the following set of balance equations:

$$\rho\dot{\boldsymbol{v}} = \boldsymbol{b} + \operatorname{div} \boldsymbol{\sigma}, \qquad \sigma = 2\rho\frac{\partial\Psi}{\partial\boldsymbol{B}_e}\boldsymbol{B}_e \tag{5}$$

$$\boldsymbol{n} \times \big(\boldsymbol{g} - \rho\frac{\partial\Psi}{\partial\boldsymbol{A}}\boldsymbol{n}\big) = \mathbf{0} \tag{6}$$

which represent the balance of linear momentum and the balance of torques, respectively. Therefore, the Clausius-Duhem inequality requires

$$\xi = \big(\boldsymbol{\sigma}_v - \rho\frac{\partial\Psi}{\partial\boldsymbol{B}_e}\big) \cdot \boldsymbol{B}_e^{\triangledown} \geq 0 \tag{7}$$

which holds true for every $\boldsymbol{B}_e^{\triangledown}$, if the following assumption is made

$$\mathbb{D}(\boldsymbol{B}_e^{\triangledown}) = \boldsymbol{\sigma}_v - \rho\frac{\partial\Psi}{\partial\boldsymbol{B}_e} \tag{8}$$

where $\mathbb{D}$ is a fourth-order positive definite tensor. Equation (8) represents an evolution equation for the elastic deformation $\mathbf{F}_e$. In order to solve it, a constitutive equation for the active stress $\boldsymbol{\sigma}_v$ must be provided; possible choices were presented in [6, 7], for nematic elastomers and anisotropic fluids, respectively. Equations (5)-(6) together (8) define the equilibrium of the nonlinear viscoelastic solid. The evolution equation of the elastic strain is a nonlinear differential equation that can be solved numerically. However, when the material reorganization is much faster than the deformation, one could recover a linear evolution equation that gives the classical Cauchy stress of a viscous fluid. On the other hand, a second order expansion of the remodelling equation around the passive equilibrium solution gives the classical nonlinear Maxwell model [8, 9, 10].

References

[1] J. Ciambella, P. Nardinocchi, *Torque-induced reorientation in active fibre-reinforced materials*, Soft Matter **15** (2019), 2081–2091.

[2] G.A. Holzapfel, T.C. Gasser, *A viscoelastic model for fiber-reinforced composites at finite strains: Continuum basis, computational aspects and applications*, Comput. Methods Appl. Mech. Eng. **190** (2001), 4379–4403.

[3] Y.C. Fung, *Elasticity of soft tissues in simple elongation*, Am. J. Physiol. **213** (1967), 1532–1544.

[4] A. Hanyga, M. Seredynska, *Multiple-integral viscoelastic constitutive equations*, Int. J. Non. Linear. Mech. **42** (2007), 722–732.

[5] M.B. Rubin, S.R. Bodner, *Modeling nonlinear dissipative response of biological tissues*, Int. J. Solids Struct. **41** (2004), 1739–1740.

[6] S.S. Turzi, *Viscoelastic nematodynamics*, Phys. Rev. E **94** (2016), 062705.

[7] K.R. Rajagopal, A.R. Srinivasa, *Modeling anisotropic fluids within the framework of bodies with multiple natural configurations*, J. Nonnewton. Fluid Mech. **99** (2001), 109–124.

[8] J. Ciambella, A. Paolone, S. Vidoli, *A comparison of nonlinear integral-based viscoelastic models through compression tests on filled rubber*, Mech. Mater. **42** (2010), 932–944.

[9] J. Ciambella, A. Paolone, S. Vidoli, *Memory decay rates of viscoelastic solids: not too slow, but not too fast either*, Rheol. Acta **80** (2011), 661–674.

[10] J. Ciambella, A. Paolone, S. Vidoli, *Identification of the viscoelastic properties of soft materials at low frequency: Performance, ill-conditioning and extrapolation capabilities of fractional and exponential models*, J. Mech. Behav. Biomed. Mater. **37** (2014), 286–298.

Linearly polarised waves in pre-strained elastic materials

Luigi Vergori

The propagation of waves in elastic materials has been investigated extensively for many decades. Nevertheless, the existence and uniqueness of solutions to Cauchy problems governing the wave propagation in a solid represent still nowadays an extremely challenging problem in nonlinear elasticity.

To the best of our knowledge, the best-so-far approaches to tackle the existence of Cauchy problems related to the wave propagation in three-dimensional nonlinearly elastic solids are based on the Glimm scheme and its variants, or the method of compensated compactness. These methods have however produced results only in very special cases. Concerning the full three-dimensional equations, very little is known with the desirable detail.

Small amplitude waves. The difficulty of solving the full nonlinear three-dimensional equations of wave propagation in elastic solids has been one of the reasons for the development of the theory of incremental motions. In this theory a wave is regarded as an infinitesimal perturbation superposed to a finite static deformation of an elastic material. The concept of incremental motions was introduced in the pioneering paper by Hayes and Rivlin [7], and since then the theory of small-on-large elastic deformations has been refined by several authors. The small-on-large theory has revealed effective not only to analyze the stability of equilibria in solid mechanics (see, for instance, the works of Destrade, Ogden and co-workers

[3, 4, 15] and references therein), but also to studying the propagation of shear waves generated by acoustic radiation forces in soft tissues [8, 9, 10].

Recently, we have shown that the incremental theory can be adopted to test whether or not a given strain energy function is good enough to model the elastic response of a material. In [13] we discuss the appropriateness of modelling brain tissue as a Mooney-Rivlin material by recurring to some identities derived within the theory of small-on-large deformations.

Simple shear tests performed on small rectangular fresh samples of porcine brain at quasi-static strain rates revealed a linear shear stress-shear strain relationship over a significant range of amount of shear (up to 60% of strain) [2]. In view of this linear relationship, brain tissue is often modelled as a Mooney-Rivlin material. However, as pointed out by Mangan *et al* [11], a strain energy function in the form

$$W = \frac{C_{10}}{2}(I_1 - 3) + \frac{\mu - C_{10}}{2}(I_2 - 3) + \hat{H}(I_1 - I_2), \tag{1}$$

with C_{10} and C_{01} being constants, I_1 and I_2 the first two principal invariants of the left Cauchy-Green deformation tensor, and $\hat{H}$ an arbitrary smooth response function depending on $I_1 - I_2$, allows the linear relationships between shear stress and shear strain in simple shear tests. Clearly, for $\hat{H} \equiv 0$ the strain energy density (1) reduces to the Mooney-Rivlin model. That is why the strain energy function (1) is known as generalized Mooney-Rivlin (GMR) model, and the corresponding class of elastic solids is said to be constituted by GMR materials.

It is therefore natural to wonder whether a GMR model with a non-identically vanishing $\hat{H}$ might lead to a deeper interpretation of the experimental data than on using the Mooney-Rivlin model. To give an answer, one can resort to the pseudo-universal relations for GMR materials which relate the speeds of small-amplitude shear waves propagating in a pre-strained material. In this talk we will show how these relations serve as necessary conditions for the strain energy function of an incompressible, isotropic hyperelastic solid to be modelled through (1), and help with the introduction of the response function $\hat{H}$ which fits best the experimental data.

Finite amplitude waves. In 2003 Catheline et al [1] reported the first experimental observation of a shock transverse wave propagating in an elastic medium. The shock formation was observed in Agar powder (3%) in suspension in a solid gelatin solution (3%) thank to an ultra-fast scanner able to acquire 5000 frames per second. The experimental data recorded are in good agreement with the theoretical predictions based on the modified Burger's equation derived for the propagation of plane transverse waves in nonlinear Kelvin-Voigt materials. One year later Sack *et al* [14] used magnetic resonance elastography to observe nonlinear shear waves and deduce from their shapes valuable information about the nonlinear stress-strain behaviour of soft tissues.

Differently from the analyses and simulations conducted by Li and co-workers [9, 10] which are based on the incremental equations of motion, the experimental data and theoretical predictions contained in [1] have been obtained by considering

waves of small-but-finite (and not infinitesimal) amplitude. Recently, the approach of Catheline *et al* [1] has been adopted to study the internal deformation of brain from an impact. Espíndola *et al* [5] considered linearly-polarised waves of small-but-finite amplitude to obtain valuable information about the nonlinear stress-strain behavior of brain tissue. This means that non-linear acoustic methods have a potential to improve non-destructive diagnostic of soft tissues. In this framework it is therefore of fundamental interest to study *small-but-finite-on-large* motions as the investigation of wave propagation on a given static pre-stretch may enlarge the horizon of experimental evaluations.

Within the theory of small-superposed-on-finite deformations, Fu and Ogden [6] explain thoroughly the analytical scheme to study the nonlinear stability of equilibrium configurations of hyperelastic bodies. The standard procedure is to study the evolution in time of a perturbation in the form of a small-amplitude (say $\mathcal{O}(\epsilon)$, with $|\epsilon| \ll 1$) travelling wave. The linear theory provides only the wave modes and the conditions under which no perturbation propagates through the pre-strained material. The wave amplitude, which cannot be determined from the linear theory, is instead to be obtained from a weakly nonlinear stability analysis in which the wave amplitude is assumed to depend on the slow-time variable $\tau = \epsilon t$. By following a similar approach in [12] we have studied the wave propagation of *finite* amplitude in a pre-strained incompressible hyperelastic solid with the clear intention to provide experimentalists a precise and feasible guidance to new experimental settings for the investigation of nonlinear effects and the determination of some elastic moduli of solids.

The objective of this part of the talk is threefold. Firstly, we focus on the necessary conditions for linearly polarized transverse waves of finite amplitude to propagate in a pre-strained incompressible hyperelastic solid. We shall show that these waves can propagate only if the cross product of the directions of polarization and propagation is a principal direction of the left Cauchy-Green deformation tensor associated with the pre-strained state (which, for the sake of brevity, is denoted $\bar{\boldsymbol{B}}$ in what follows). This means that linearly polarized transverse waves of finite amplitude can propagate only in principal planes of $\bar{\boldsymbol{B}}$. Secondly, we show that, when the wave amplitude is much smaller than the maximum displacement from the reference configuration in the pre-strained state, depending on the angle subtended by the direction of propagation and the principal directions of $\bar{\boldsymbol{B}}$ the nonlinear effects become important at time-scales of different orders. Finally, we shall design theoretically a procedure aiming at the determination of the Landau constants of the fourth-order weakly nonlinear theory of elasticity.

References

[1] S. Catheline, J.L. Gennisson, M. Tanter, M. Fink, *Observation of shock transverse waves in elastic media*, Phys. Rev. Lett. **91**(2003), 164301.

[2] M. Destrade, M.D. Gilchrist, J.G. Murphy, B. Rashid, G. Saccomandi, *Extreme softness of brain matter in simple shear*, International Journal of Non-Linear Mechanics **75** (2015), 54–58.

[3] M. Destrade, R.W. Ogden, I. Sgura, L. Vergori, *Straightening wrinkles*, J. Mech. Phys. Solids **65**(2014), 1–11.
[4] M. Destrade, R.W. Ogden, I. Sgura, L. Vergori, *Straightening: existence, uniqueness and stability*, *Proc. R. Soc. A* **470** (2014), 20130709.
[5] D. Espíndola, S. Lee, G. Pinton, *Shear Shock Waves Observed in the Brain*, Phys. Rev. Applied **8** (2017), 044024.
[6] Y.B. Fu, R.W. Ogden, *Nonlinear stability analysis of pre-stressed elastic bodies*, *Continuum Mech. Therm.* **11** (1999), 141–172.
[7] M. Hayes, R.S. Rivlin, *Propagation of a plane wave in an isotropic elastic material subjected to pure homogeneous deformation*, *Arch. Ration. Mech. Anal.* **8** (1961), 15–22.
[8] Y. Jiang, G.Y. Li, L.X. Qian, X.D. Hu, D. Liu, S. Liang, Y. Cao, *Characterization of the nonlinear elastic properties of soft tissues using the supersonic shear imaging (SSI) technique: Inverse method, ex vivo and in vivo experiments*, *Med. Image Anal.* **20** (2015), 97–111.
[9] G.Y. Li, Y. Zheng, Y. Liu, M. Destrade, Y. Cao, *Elastic Cherenkov effects in transversely isotropic soft materials-I: theoretical analysis, simulations and inverse method*, J. Mech. Phys. Solids **96** (2016), 388–410.
[10] G.Y. Li, Q. He, L.X. Qian, H. Geng,Y. Liu, X.Y. Yang, J. Luo, Y. Cao, *Elastic Cherenkov effects in transversely isotropic soft materials-II: ex vivo and in vivo experiments*, Journal of the Mechanics and Physics of Solids**94** (2016), 181–190.
[11] R. Mangan, M. Destrade, G. Saccomandi, *Strain energy function for isotropic non-linear elastic incompressible solids with linear finite strain response in shear and torsion*, Extreme Mechanics Letters **9** (2016), 204–206.
[12] E. Pucci, G. Saccomandi, L. Vergori, *Linearly polarised waves of finite amplitude in pre-strained elastic materials*, submitted.
[13] G. Saccomandi, L. Vergori, *Generalised Mooney-Rivlin models for brain tissue: a theoretical perspective*, Int. J. of Nonlin. Mech. **109**(2019), 9–14.
[14] I. Sack, C.K. Mcgowan, A. Samani, C. Luginbuhl, W. Oakden, D.B. Plewes, *Observation of nonlinear shear wave propagation using magnetic resonance elastography*, *Mag. Reson. Med.* **52** (2004), 842–850.
[15] T. Sigaeva, R. Mangan, L. Vergori, M. Destrade, L. Sudak, *Wrinkles and creases in the bending, unbending and eversion of soft sectors Proc. R. Soc. A* **474**(2018), 20170827.

Reporter: Luigi Vergori

Participants

Prof. Dr. Valentina Balbi
Mathematics Department
National University of Ireland, Galway
University Road
Galway H91 TK33
IRELAND

Prof. Dr. Miroslav Buliček
Mathematical Institute
Charles University
Sokolovska 83
186 75 Praha 8
CZECH REPUBLIC

Prof. Dr. Jacopo Ciambella
Department of Structural and Geotechnical Engineering
Università di Roma "La Sapienza"
Via Eudossiana 18
00184 Roma
ITALY

Prof. Dr. Michel Destrade
School of Mathematics, Statistics and Applied Mathematics
National University of Ireland, Galway
University Road
Galway H91 TK33
IRELAND

Prof. Dr. Hüsnü A. Erbay
Department of Natural and Mathematical Sciences
Faculty of Engineering
Özyegin University
Nisantepe, Orman Sk. No: 13
Cekmeköy 34794 / Istanbul
TURKEY

Prof. Dr. Yibin Fu
Department of Mathematics
University of Keele
Keele, Newcastle, Staffs ST5 5BG
UNITED KINGDOM

Prof. Dr. Katrin Grunert
Department of Mathematical Sciences
NTNU
Alfred Getz vei 1
7491 Trondheim
NORWAY

Dr. Anastasiia Krushynska
Noweestraat 39
6708 TN Wageningen
NETHERLANDS

Dr. Andrea Nobili
Department of Engineering "Enzo Ferrari"
University of Modena and Reggio Emilia
Via Vivarelli 10
41125 Modena
ITALY

Dr. Ilya M. Peshkov
Institut de Mathématiques de Toulouse
Université Paul Sabatier
118, route de Narbonne
31062 Toulouse Cedex 9
FRANCE

Prof. Dr. Gianmarco Pinton
Department of Mathematics
University of North Carolina at Chapel Hill
Phillips Hall
Chapel Hill, NC 27599-3250
UNITED STATES

Prof. Dr. Giuseppe Saccomandi
Dipartimento di Ingegneria
Università degli Studi di Perugia
Via G. Duranti, 1
06125 Perugia
ITALY

Prof. Dr. Yasemin Sengül Tezel
Faculty of Engineering and Natural Science
Sabanci University
Orhanli
34956 Tuzla/Istanbul
TURKEY

Prof. Dr. Athanasios E. Tzavaras
Applied Mathematics and Computational Sciences
4700 King Abdullah University of Science
and Technology (KAUST)
Thuwal 23955-6900, Jeddah
SAUDI ARABIA

Prof. Dr. Luigi Vergori
Dipartimento di Ingegneria
Università degli Studi di Perugia
Via G. Duranti, 1
06125 Perugia
ITALY